ABSTRACT

Title of Document: EFFECT OF FREE CHLORINE OXIDATION ON THE DEPOSITION KINETICS OF BACTERIOPHAGE MS2 ON A SILICA SURFACE

Heungkook Noriomoral Stephens, Master of Science, 2015

Directed By: Professor Baoxia Mi, Department of Civil and Environmental Engineering

Understanding the transport kinetics of water contaminates such as pathogenic viruses around solid surfaces is important in controlling groundwater contaminant plumes and optimizing contaminant removal in sand filtration units. The effect of increasing oxidative stress, in the form of small doses of free chlorine, on the deposition behavior of bacteriophage MS2 onto a silica surface was examined using a quartz crystal microbalance with dissipation (QCM-D). MS2 deposition rates were analyzed by reaction time and inactivation level. A statistically significant increase in the deposition rate was identified between MS2 test solutions not exposed to free chlorine and most test solutions that were exposed. However, as exposure to free chlorine was increased, no relationship was able to be deduced from the collected deposition data. Potential explanations based on previous work were discussed. Observations also indicated that more comprehensive purification procedures in comparison to previous studies were necessary to obtain accurate QCM-D data.

EFFECT OF FREE CHLORINE OXIDATION ON THE DEPOSITION KINETICS OF BACTERIOPHAGE MS2 ON A SILICA SURFACE

By

Heungkook Noriomoral Stephens

Thesis submitted to the Faculty of the Graduate School of the
University of Maryland, College Park, in partial fulfillment
of the requirements for the degree of
Master of Science
2015

Advisory Committee:
Professor Baoxia Mi, Chair
Professor Alba Torrents
Professor Birthe Kjellerup

Dedication

To my friends and family, especially my beautiful wife, Jin Soon, for their support and inspiration. This was part of a larger journey I hope to continue with all of you.

Acknowledgements

A very special thanks to Dr. Krista Wigginton for her mentorship and care from near and far, for always being understanding and encouraging, and for pushing me and looking out for me.

Thank you to the members of my committee, Dr. Allen Davis, Dr. Birthe Kjellerup, and notably Dr. Baoxia Mi for chairing my committee.

Thank you to my lab mates for being great friends and support, especially Eric Liang whose support extended even further into my career. Finally, thank you to the department staff, including Al Santos, who was always willing to offer wisdom and good conversation.

Table of Contents

List of Tables

List of Figures

Chapter 1: Introduction

1.1 Waterborne Viruses

Viruses are the most abundant biological entity on the planet. Their genetic elements are nanometers in scale. Viruses are usually not considered living organisms because they do not have a cellular structure and do not have their own metabolism. Virus particles consist of just a few parts; their genetic material consisting of either DNA or RNA, a protein capsid structure that houses the genetic material, and a lipid outer layer that is present in some types of viruses. Waterborne viruses rarely have a lipid envelope though (Cliver & Moe, 2004). To survive and multiply, viruses must infect a host cell and use the metabolism and structure of the host cell to synthesize the proteins coded in its genome. There are viruses that infect all types of cellular organisms, including the different cells within the human body. Because viruses take over the protein synthesis function of the host cell, viral infection can be destructive to the host organism, have a pathogenic effect, and result in disease. Viral disease can be spread through several means, including droplet contact (coughing or sneezing through the air), direct contact, bodily fluids, and oral ingestion of fecal-contaminated food or water. There are several viruses that are spread through the fecal-oral route. The following table summarizes the characteristics of four such viruses. These viruses are often characterized as waterborne viruses, as they are readily transmitted via contaminated water.

Virus Species	Disease	General Symptoms	Notes
Norovirus	viral gastroenteritis	Nausea, vomiting, diarrhea, fever, abdominal pain	267 million infections/year worldwide; 200,000 child deaths/year in developing countries (Debbink, Lindesmith, Donaldson, & Baric, 2012).
Rotavirus	viral gastroenteritis	Nausea, vomiting, diarrhea, fever, abdominal pain	Mainly in young children; 453,000 children under age 5 died from infection worldwide in 2008 (Tate, et al., 2012).
Poliovirus	Poliomyelitis (Polio)	Fever, fatigue, headache, vomiting, stiffness, pain	Can invade the nervous system and cause paralysis; poliomyelitis cases have been reduced by over 99% since 1988 thanks to vaccination. (World Health Organization, 2014)
Hepatitis A Virus	Hepatitis A	Fatigue, fever, nausea, Jaundice (a yellowing of the skin or whites of the eyes due to hyperbilirubinemia)	In the United States, there were an estimated 25,000 new Hepatitis A virus infections in 2007, but could be higher since many people who are infected never have symptoms (Centers for Disease Control and Prevention, 2013)

Table 1: Fecal-Oral Transmitted Viruses

1.2 Viral Transport through Groundwater

1.2.1 Groundwater and Groundwater Contamination

Groundwater resides in the pore space between soil particle and rock formations in the subsurface. These water-carrying formations are known as aquifers. Groundwater travels through aquifers very slowly, measured in a range between days to centuries depending on the depth and location (Winter, Harvey, Franke, & Alley, 2013). Groundwater is usually considered clean and potable because of the natural purification that takes place in the subsurface such as sorption-desorption, oxidation-reduction, and biodegradation. Ground water is therefore typically an excellent source of freshwater for municipal, agricultural, and industry needs (Balke & Zhu, 2008). About half of the United States population relies on groundwater drawn up through wells as their primary drinking water source (Loveland J. , Ryan, GL, & RW, 1996). Groundwater is vulnerable to contamination from a variety of sources including leaking septic tanks, sewage lines, and landfills. Agricultural practices that pollute surface water can also eventually contaminate groundwater sources (Böhlke, 2002).

When a pollutant enters a layer of groundwater, it creates a plume that can eventually contaminate the entire aquifer (Fetter, 1999). Only about half of all public groundwater systems are disinfected, so groundwater contamination by waterborne pathogens can be very dangerous to public health (Berger & Zoller , 1994). In fact, one-third of all waterborne disease outbreaks in recent decades was a result of untreated groundwater (Loveland J. , Ryan, GL, & RW, 1996). A majority of recent outbreaks associated with groundwater contamination have been associated with pathogenic viruses, which have been found in both groundwater and well water (Tong, Shen, Yang, & Kim, 2012).

1.2.2 Factors Influencing Viral Transport in Groundwater

It is important to understand viral transport in groundwater to predict and control potential viral outbreaks. The same understanding can also help predict the effectiveness of sand filters in removing viruses. Among microscopic biological entities, viruses typically have very conservative and predictable transport behavior (Loveland J. , Ryan, GL, & RW, 1996). Virus transport in groundwater is controlled by many factors including advection, dispersion, and deposition and detachment from soil surfaces. The movement of viruses in groundwater is directly controlled by how they interact with solid surfaces, and therefore it is important to understanding the mechanisms of virus attachment to solid surfaces (Yuan, Pham, & Nguyen, 2008). The deposition behavior of viruses in groundwater is affected by several factors such as flow velocity and temperature (Tong, Shen, Yang, & Kim, Deposition kinetics of MS2 bacteriophages on clay mineral surfaces, 2012), along with several intermolecular forces, the properties of the soil, and the virus structure itself.

Electrostatic Forces

Electrostatic forces play a large role in the deposition behavior of viruses in groundwater (Loveland J. , Ryan, Amy, & Harvey, 1996). Electrostatic forces can be explained using the electrical double layer theory. In this theory, a solution contains both positively and negatively charged ions, which give the solution an overall electro-neutral charge. All particles have some sort of surface charge that will gather ions around in with the opposite charge. Typically, a colloid particle in a solution has a negative charge and will gather positively charged ions around it, creating a layer of positively charged ions around itself. The farther the distance from the colloid, the weaker the electric charge of the layer. In addition, the charged layer surrounding the

colloid particles will repel the particles away from each other. If the charged layer around the colloid is relatively thin, then counter attractive forces such as Van der Waals forces, can overpower the weaker repellent electrostatic force, allowing the colloid particles to attach to each other and to other surfaces. Increasing the ionic strength of a solution is one way to decrease the "thickness" of the ion layer, allowing for counter attractive forces to dominate (Russel, Saville, & Schowalter , 1992). Changes in pH also have an effect on the electrostatic properties of a colloid. Decreasing pH (i.e., increasing the concentration of hydrogen atoms in the solution) promotes protonation of the colloids' surface, thus making their charge less negative. When the pH drops to what is called the isoelectric point of a particle, the particle has a neutral charge. Having a neutral charge leads to aggregation of the colloid particles and adsorption of the particles to surfaces. In general, colloid particles have a negative charge above their isoelectric point, and a positive charge below their isoelectric point.

Hydrophobic Interactions

Hydrophobic interactions also play a significant role in the deposition behavior of viruses (Voorthuizen, Ashbolt, & Schäfer, 2001). Molecules have a tendency to exhibit either polar or non-polar characteristics depending on their functional groups (Brewer, Glomm, Johnson, Knag, & Franzen, 2001). A functional group will exhibit polar characteristics if there is an unequal distribution of its electrons over its molecular structure, as is the case with hydroxyl, carboxyl, and amino groups, all common in biological molecular structures. These functional groups are considered hydrophilic. A functional group will exhibit non-polar characteristics if there is an even distribution of its electrons, as is the case with methyl and phenyl groups, also common in biological molecular structures (Ophardt, 2003b). These functional groups are considered

hydrophobic. Functional groups have varying levels of polarity and thus hydrophobicity. The hydrophobic effect is the tendency for particles with more non-polar characteristics to repel water in a solution (water being a polar substance) and aggregate with themselves. Hydrophobic particles constructed from hydrophobic molecules and functional groups tend to adsorb more easily to hydrophobic surfaces in water, while hydrophilic particles made from hydrophilic molecules and functional groups tend to dissolve and resist aggregating. Voorthuizen et al. reinforced the importance of hydrophobicity in the deposition behavior of viruses through their study of the retention of the bacteriophage MS2 using hydrophobic (GVHP) and hydrophilic (GVWP) 0.22 μm MF membranes which revealed that retention was much greater on the hydrophobic membrane (2001).

Soil Properties

The characteristics of the soil surface affects the nature of the virus deposition behavior in groundwater (Rechendorff, Hovgaard, Foss, Zhdanov, & Besenbacher, 2006). Soil is primarily made of sand, silt, clay, and organic matter. Clays, in particular, are composed of aluminum and silica. Clay particles naturally have a negative charge due to isomorphous substitution, or the substitution of one element for another characteristically similar element in an ionic crystal without changing the structure. The Al^{3+} in the clay is substituted for Si^{4+}, and because Si^{4+} has an additional electron, the overall charge becomes negative. This charge is not pH dependent, and will be present regardless of the solution chemistry (Donahue, Miller, & Shi, 1977). Silica is also naturally hydrophilic (Laskowski & Kitchener, 1969).

Virus Structure

The properties of the virus structure control the nature of the interaction between the virus particle and soil surface. It can be assumed that the capsid structure will primarily influence the deposition behavior of a virus since it is the only portion of the particle exposed to the solution (Penrod, Olson, & Grant, 1996). The capsid is made of proteins, which are composed of amino acids. There are 20 standard amino acids that combine to form proteins, each being composed of an amino group, a carboxyl group, a central alpha carbon, and an R-group or side chain. Amino acids come together in a long chain called a polypeptide, bonded by peptide bonds between their amino and carboxyl groups. The polypeptide minus the side chains is known as the protein backbone. An amino acid's charge, isoelectric point, and hydrophobicity are largely influenced by its side chain. Based on the hydrophobicity, charge, and order of the amino acids in the polypeptide chain, polypeptides fold onto themselves to form secondary structures such as alpha helices and beta sheets. These secondary structures then further fold into each other to form the tertiary structure of the complete protein. These full proteins interact to form the virus particle, or quaternary structure.

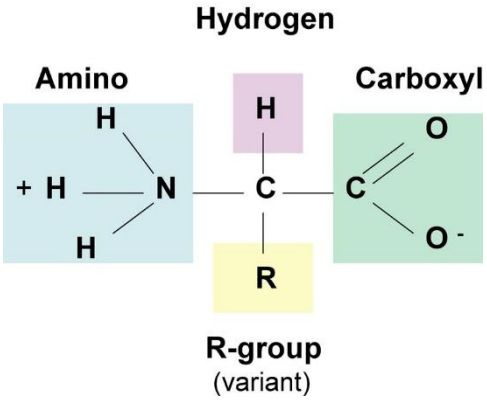

Figure 1: Diagram of the structure of an amino acid *(Amino Acids, 2013).*

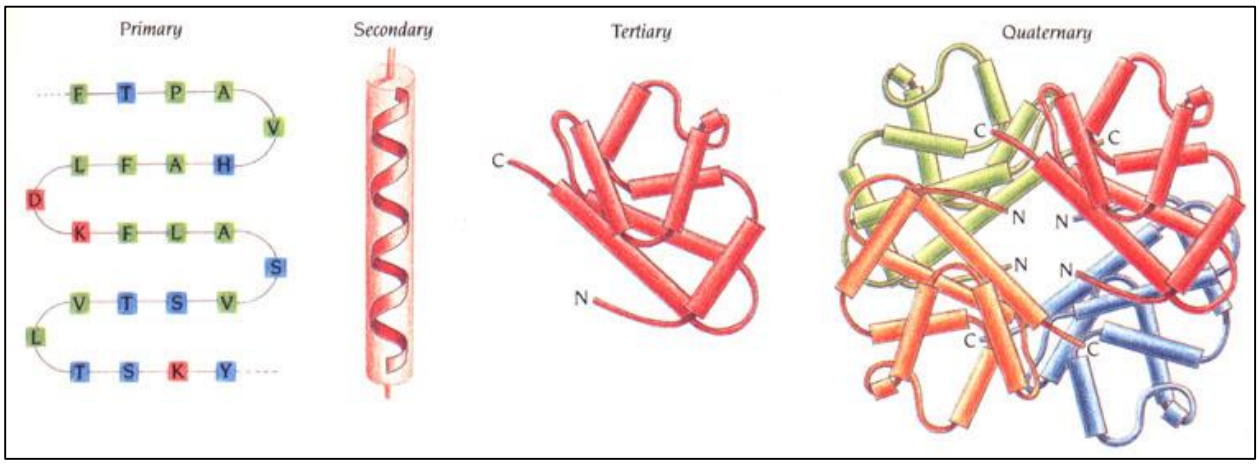

Figure 2: Diagrams showing the levels of protein structure *(Proteins, 2007-2015).*

In addition to the collective properties of the amino acids making up the protein, the secondary and tertiary structure of each protein, and the quaternary structure of the virus capsid, play a large role in the overall characteristics of the virus capsid structure (Penrod, Olson, & Grant, 1996). Rarely is it true that a simple average of the measurable characteristics of all the amino acids in the virus protein capsid explains the overall behavior of a virus. This is because of the heterogeneous structure of a virus. Distinct parts or sections of the protein that have specialized functions such as host attachment can have a specific charge or hydrophobicity that differs from the overall capsid. In a virus capsid, the characteristics of the exposed capsid may be very different from the characteristics of the inside of the capsid (Penrod, Olson, & Grant, 1996). In general, viruses tend to have isoelectric points below natural water pH, and therefore commonly have negative charges in the natural environment (Michen & Graule , 2010).

1.3 The Effect of Oxidative Stress on Viral Transport in Groundwater

One naturally and unnaturally occurring variable whose effect on viral deposition and transport that has not yet been explored extensively is oxidative stress. Viruses outside of a

laboratory environment encounter multiple sources of oxidative stress. Many reactive oxidative sources naturally exist in natural waters including ultra violet light, singlet oxygen, ozone, and hydrogen peroxide (Stadtman, 1992). Water treatment also introduces oxidative stress on viruses. Chlorine, for example, is used to disinfect drinking water in treatment plants both as a primary disinfectant and as a residual disinfectant. Chlorine is also used to treat wastewater before it is quenched and released into natural bodies of water. Studies that examine virus particle transport have historically employed "fresh" viruses that were recently propagated in laboratory cell systems. As a result, these viral stocks used for studying virus sorption and transport behavior were not exposed to oxidative species that viruses in the environment have likely encountered.

Oxidants react with the molecular structure of the virus' genetic material and proteins, producing radicals and damaging the virus. In general, disinfectants inactivate viruses by inhibiting the virus' ability to bind to a host organism, to inject its genetic material into the host, and/or to replicate its genome. Inactivation is a result of the loss of one or more of these functions. Disinfectants react with the virus proteins and genomes, eventually disabling one of the necessary functions. The damaged structure and the eventual inhibited function depends both on the disinfectant and the virus in question. Certain virus structures can be more reactive to different disinfectants compared to other virus structures. However, those more reactive structures are not necessarily the eventual cause of inactivation depending on the complex series of reactions (Wigginton, Pecson, Sigstam, Bosshard, & Kohn, 2012). Therefore, even though oxidants, especially chlorine, damage viruses, viruses can remain infective after certain levels of exposure (Centers for Disease Control and Prevention, 2009).

Consequently, the behavior of oxidized, but not inactivated viruses is important to understand. Viruses tend to aggregate into clumps in the environment or into surfaces (Narang &

Codd, 1981). This aggregation inhibits disinfection because viruses on the outer layer of the aggregate protect the viruses towards the center of the aggregate from reacting with oxidants (Mattle, et al., 2011). In addition, some types of viruses are more resistant to disinfectants than others, and may require more contact time with disinfectant than the actual dose amount in a particular situation. For example, Hepatitis A virus takes about 16 minutes at 1 mg/L chlorine to be disinfected compared to the 3 seconds at 1 mg/L chlorine it takes to disinfect rotavirus (Centers for Disease Control and Prevention, 2010) (Hoff, 1986). Consequently, oxidative stresses in the environment may lead to only slightly oxidized capsid proteins without fully inactivating the virus.

1.3.1 Characteristics and Behavior of Free Chlorine

Chlorine has long been used as an effective means of water disinfection. Chlorine is a very reactive oxidant because it has seven electrons in its outer orbital and only requires one more to become complete. It easily develops covalent bonds with atoms in organic compounds by replacing hydrogen atoms. Many different forms of chlorine are used in water treatment such as chlorine gas (Cl_2) and hypochlorous acid (HOCl, applied as sodium hypochlorite or calcium hypochlorite). When chlorine gas is added to water, it transforms to hydrochloric acid and hypochlorous acid. Because hydrochloric acid is a strong acid, it quickly dissociates into H^+ and Cl^-. Hypochlorous acid, a weak acid, maintains an equilibrium between HOCl and hypochlorite ($-OCl^-$) with a pK_a of 7.53. Together, these reactive chlorine species in water are called free chlorine (FC). HOCl is the more reactive form and therefore, free chlorine is more reactive at lower pH values.

1.3.2 Expected Effects of Free Chlorine on Viruses

The amino acid side chains and the protein backbones of virus capsids are the primary targets of oxidation (Pattison, Hawkins, & Davies, 2007). Oxidation via free chlorine results in the formation of radicals and chloramines, which can react further with the oxidant or with other amino acids. These reactions can lead to crosslinking and fragmentation along the protein backbone (Hawkins & Davies, 1998b).

Certain amino acid side chains and protein backbone groups are more reactive than others; allowing one to potentially predict the overall series of reactions that might take place with a virus protein capsid (Hoff, 1986). The order of reactivity with hypochlorous acid/free chlorine, with the most reactive protein components listed first, is provided below:

Amino Acid/Protein Structure	2nd Order Rate Constant with HOCl [k (M^{-1} s^{-1})]
Amino acid side chains that contain sulfur	
Methionine	3.8×10^7
Cysteine	3.0×10^7
Ends of the polypeptide chains	
Alpha amino group	1.0×10^5
N-terminal group	1.0×10^5
Amino acid side chains with reactive functional groups	
Lysine (amino group)	5.0×10^3
Tyrosine (hydroxide group)	4.4×10^1
Protein Backbone	1.0×10^1
Other side chains	$< 1.0 \times 10^1$

Table 2: Reported 2nd Order rate constants for reactive amino acids and protein structures with free chlorine at pH ~7 *(Pattison & Davies, 2001).*

In general, oxidation will not change the charge state of the effected molecules; therefore, any changes in adsorption behavior due to oxidation are not due to electrostatics. Reactions with

bleach cause viruses or pieces of viruses to aggregate (Jakob, Muse, Eser, & Bardwell, 1999), which may be due to an increase in protein crosslinking or hydrophobicity. However, the series of reactions that takes place at the virus capsid under oxidative stresses below inactivation levels depends greatly on the specific virus being considered.

1.4 Bacteriophage MS2

When researching virus behavior in the environment or in engineered systems, surrogate viruses are often employed. One reason for the use of surrogate viruses is that not every human virus can be cultured in a laboratory. For example, norovirus does not replicate sufficiently in available cell culture systems (Steinmann, 2004). Surrogate viruses are often easier to culture to high concentrations and do not have the associated biosafety issues of pathogenic viruses. Surrogate viruses can be selected with structural properties that are similar to the virus of interest. MS2, for example, is a virus that infects bacteria (i.e., bacteriophage) and is commonly used as a surrogate for enteric viruses such as norovirus (Dawson, Paish, Staffell, Seymour, & Appleton, 2005). The protein structure of MS2 is well established (The UniProt Consortium, 2015), as well as its inactivation pathways with free chlorine (Wigginton, Pecson, Sigstam, Bosshard, & Kohn, 2012). The comprehensive knowledge of MS2 leads it to be an excellent choice for studying viral transport along with the effects of oxidation on viral deposition behavior.

1.4.1 Structure of MS2

MS2 is an icosahedral, positive-sense single-stranded RNA virus that infects the bacterium *Escherichia coli* (Brinton, Gemski, & Carnahan, 1964). The virus particle is made of

three structures: the genome, a single copy of the assembly protein, and 180 copies of the capsid protein. The capsid proteins create the virus shell that encompasses the genome. The capsid proteins, and namely their external parts, likely govern the transport behavior of the virus through groundwater. The capsid proteins are organized into 90 dimers and 60 identical triangular units. Each protein is made of 129 amino acids. These amino acids fold into 7 beta sheets and 2 alpha helices. When the entire capsid comes together, for each individual protein, beta sheets βA and βB along with both alpha helices are located on the exterior of the capsid (Golmohammadi, Valegård, Fridborg, & Liljas, 1993).

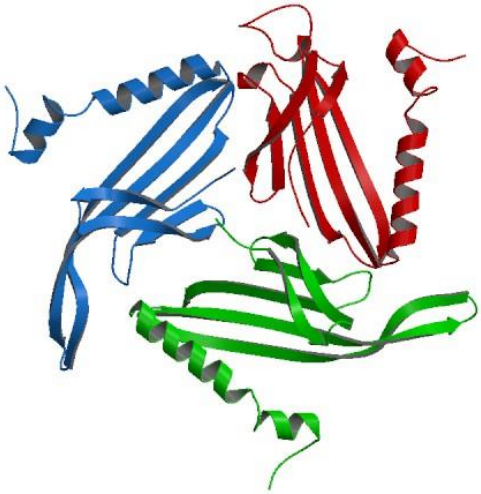

Figure 3: Diagram of one of the 60 triangular units *(Bacteriophage MS2 (MS2), 2015).*

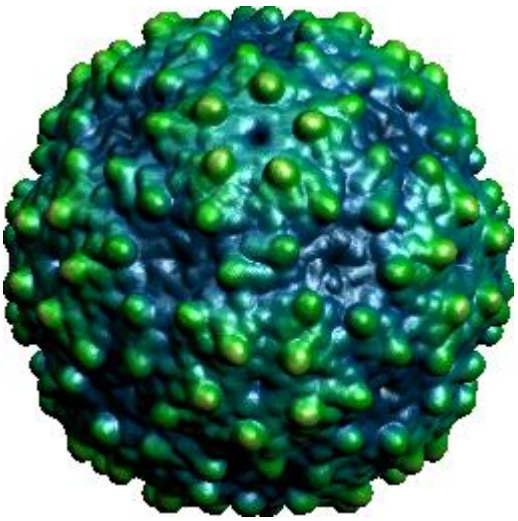

Figure 4: Diagram of Bacteriophage MS2, showing the complete protein capsid structure *(Bacteriophage MS2 (MS2), 2015).*

There are distinct differences between the properties of the capsid protein interior and exterior. Based on averaging the hydropathy index of the amino acids composing the interior and exterior of the capsid structure, the interior is overall hydrophilic while the exterior is overall hydrophobic (The UniProt Consortium, 2015). MS2 is particularly hydrophobic (Farkas, Varsani, & Pang, 2014). An unusual structural characteristic of MS2 is the presence of exterior hydrophilic polypeptide loops that connect various secondary structures and protrude out one nanometer from the capsid (Valegård, Liljas, Fridborg, & Unge, 1990). When considering all structures that make up the MS2 virus, including the nucleic acids, the overall observed isoelectric point is above pH 9; however, the exterior capsid surface has an isoelectric point closer to the empirically measured value of 3.9 (Penrod, Olson, & Grant, 1996). The isoelectric point of viruses that replicate in plants, animals, or bacteria frequently falls between 3.5 and 7, so MS2 is relatively one of the more negatively charged viruses (Michen & Graule , 2010).

1.4.2 Deposition Behavior of MS2

The intermolecular forces that control the deposition behavior of the MS2 particle are complex. Due to the negative charge of MS2 and the negative charge of soil particles in natural water conditions, it would be assumed that electrostatic forces usually prevent MS2 from readily depositing onto soil surfaces. However, hydrophobic interactions also have a strong impact on MS2 deposition behavior, perhaps orders of magnitude stronger (Shields & Farrah, 2002).

At pH values near or below the isoelectric point of MS2 and under high ionic strength conditions, MS2 sorption is governed by hydrophobic forces (Loveland J. , Ryan, Amy, & Harvey, 1996). As the repellant electrostatic forces are negated, Van der Waal's forces would typically allow virus and soil particles to attract and remain in contact according to the electrical double layer theory. MS2, however, deviates from this typical behavior. It never experiences high rates of deposition, and can even experience a decrease in deposition rate at very high ionic strengths (Penrod, Olson, & Grant, 1996). The reason for this is not completely understood, but is considered the result of its unique capsid protein structure and hydrophobicity forces. In particular, the polypeptide loops protruding out of each capsid protein may prevent adsorption through steric repulsion (Penrod, Olson, & Grant, 1996).

1.4.3 Expected Effects of Chlorine Oxidation on MS2 Deposition

Correlation between log_{10} Inactivation and Capsid Protein Damage

It is expected that only the externally exposed amino acid structures will continue to govern deposition behavior following low oxidant doses that do not result in high levels of inactivation. Wigginton et al. used matrix-assisted laser desorption/ionization mass spectrometry (MALDI-MS) analysis to quantify modifications to MS2 virus structures caused by different

disinfectants, including modifications to the capsid protein caused by reacting with free chlorine. Modification of the capsid proteins was quantified by the decay rate of the capsid protein peptides. According to Wigginton et al., free chlorine causes extensive and widespread modifications to the capsid protein and greater inactivation levels (reported as $\log_{10}$ inactivation) correspond to more capsid proteins being modified. At lower levels of inactivation, the capsid protein remains mostly unaltered and intact. By 5 $\log_{10}$ inactivation, the probability that a capsid protein remained unmodified was approximately 10%. Previous work done by Wigginton et al. suggested that at 5 $\log_{10}$ inactivation, the MS2 viruses are completely broken apart. For this reason, it can be assumed that the capsid protein that governs deposition behavior steadily experiences more damage as the population of MS2 virus experiences greater $\log_{10}$ inactivation due to increased exposure to free chlorine (Wigginton, Pecson, Sigstam, Bosshard, & Kohn, 2012).

Expected Series of Reactions between Free Chlorine and Molecular Protein Structures

Based on relative reaction rates with chlorine, the side chains of methionine, cysteine lysine, and tyrosine, as well as the protein backbone are expected to react with chlorine within the timeframe of MS2 inactivation.

Methionine and cysteine are the most reactive amino acids, being over 100 times more reactive than anything else in the capsid proteins due to their sulfur containing side chains (Pattison, Hawkins, & Davies, 2007). Both of these amino acids are initially hydrophobic and uncharged. There are two methionine and one cysteine amino acids located on the exterior surface of each of the 180 MS2 capsid protein (The UniProt Consortium, 2015). The oxidation of methionine by hypochlorite results in a hydrogen atom being replaced by an oxygen atom, resulting in the formation of methionine sulfoxide, and further oxidization leads to methionine

sulfone (Pattison, Hawkins, & Davies, 2007). Typically, it would be assumed that this process would decrease hydrophobicity since the addition of an oxygen atom creates a polar, hydrophilic carboxyl functional group. However, for some proteins it has been shown that oxidation of methionine sometimes results in an increase in hydrophobicity, perhaps as a result of changes in protein conformation that lead to the exposure of hydrophobic residues (Vogt, 1995). On the other hand, the interior of the MS2 capsid protein is overall hydrophilic; therefore, it does not seem likely that protein structural changes would expose additional hydrophobic residues.

After methionine and cysteine, the next molecular protein structures expected to react with chlorine are the alpha and N-terminal amino groups (Hoff, 1986). The alpha and N-terminal amino groups are located at the ends of each polypeptide chain and both ends of the capsid polypeptide are located on the exterior of the capsid structure (The UniProt Consortium, 2015). Thus, alpha and N-terminal amino groups are also vulnerable to react with chlorine. Oxidation at either the alpha amino group or the N-terminal amino group generates unstable chloramines, NH_3, CO_2 and aldehydes (Hawkins & Davies, 1998a). Aldehydes are polar functional groups (Ophardt, Polarity of Organic Compounds, 2003b); these would therefore cause a decrease on the overall hydrophobicity of the protein.

The next most reactive structures in the capsid proteins are the lysine side chains (Hoff, 1986). Lysine is hydrophilic with a basic polar side chain. Lysine is typically positively charged at typical environmental water pH levels (pI = 9.74) (Ophardt, Characteristics and Properties of Amino Acids, 2003a) (McGraw-Hill Education, n.d.). There are two lysine amino acids located on the exterior of the capsid protein (The UniProt Consortium, 2015). The oxidation of lysine leads to a nucleophilic reaction creating semi-stable chloramine (N-Cl) species (Hawkins & Davies, 1998b). When treated with chlorine, the hydrogen atoms on the amino functional group

on the end of the side chain are replaced with chlorine atoms (Walse, Plewa, & Mitch, 2009). Because chlorine is more electronegative than hydrogen and comparable to oxygen, the chlorinated lysine can be expected to be more polar and thus less hydrophobic.

Following lysine, tyrosine is the next most reactive side chain in the MS2 capsid protein (Hoff, 1986). Tyrosine is hydrophilic and is typically uncharged or positively charged at circumneutral pH (pI = 5.66) (Ophardt, Characteristics and Properties of Amino Acids, 2003a) (McGraw-Hill Education, n.d.). Tyrosine has a phenol ring which can react with chlorine (Fu, 2000). There is one tyrosine amino acid on the exterior of the MS2 capsid protein (The UniProt Consortium, 2015). Chlorine atoms substitute hydrogen on the tyrosine phenol ring (Fu, 2000), decreasing the hydrophobicity of the side chain. When HOCl reacts with tyrosine residues, 3-chlorotyrosine (3-Cl-Tyr) and 3,5- dichlorotyrosine (3,5-Cl2-Tyr) are formed (Pattison, Hawkins, & Davies, 2007) (Ogata, 2007) (Hawkins & Davies, 2005). These products have been suggested to be stable, ceasing any further reactions (Fu, 2000). The oxidation of tyrosine also results in the formation of tyrosine-tyrosine cross-linkages, or dityrosine (Berlett & Stadtman, 1997), which can lead to protein aggregation (Dubinina, et al., 2002). The formation of dityrosine has been strongly correlated with an increase in hydrophobicity, though the direct cause is unknown (Chao, Ma, & Stadtman, 1997).

Even though these amino acids are more reactive than the protein backbone, of the 60 amino acids exposed to the exterior of each of the 180 MS2 capsid proteins, there are only 2 methionine, 1 cysteine, 2 lysine amino acids, and 1 tyrosine in addition to the two ends of the polypeptide (The UniProt Consortium, 2015). Once the chlorine demand of these molecular structures is met and they have fully reacted with free chlorine, the protein backbone may quickly begin oxidizing. Many studies have shown that a high excess of chlorine or extended

contact time is required to witness oxidation of the protein backbone (Hawkins & Davies, 1998b). However, the number of backbone amide groups in a protein is higher than any specific side chain, and therefore the reaction of chlorine with the protein backbone may be more governing with certain viruses (Pattison, Hawkins, & Davies, 2007). Backbone oxidation creates chloramine and nitrogen-centered radicals, leading to protein fragmentation, cleavage, unfolding, and/or crosslinking/aggregation (Hawkins & Davies, 1998b). In the presence of oxygen, carbon centered radicals react with each other creating cross-links. In the absence of oxygen, protein cleavage can occur (Berlett & Stadtman, 1997). The oxidation of the protein backbone can also lead to the disruption of hydrogen bonds, and thus the unfolding of protein capsid tertiary and secondary structures (Hawkins & Davies, 1998a). If cross-linking and aggregation occur, it can lead to larger sized particles. Larger proteins typically have greater deposition (Vörös, 2004), likely due to an increase in molecular weight and larger surface area for contact. If unfolding/fragmentation occur, it can lead to the hydrophilic interior structures to be exposed, decreasing the hydrophobicity of the virus.

1.5 Quartz Crystal Microbalance-Dissipation

Quartz Crystal Microbalance with Dissipation (QCM-D) is a relatively new instrument used for studying molecular interactions with a surface at a nanoscale level. It provides data on the change in mass on a crystal balance (Biolin Scientific, 2014). The basic function of the QCM-D is based on the piezoelectric effect, where the application of an electric current causes a quartz crystal to vibrate at a specific frequency (Zhang & Vetelino, 2003). A quartz crystal sensor is placed in an enclosed chamber/flow module. On one side of the sensor, an electrode applies an electric current to the sensor and the vibration frequency is measured. A solution

flows over the surface on the other side of the sensor. The solution can have any sort of chemistry and contain various organic or inorganic particulates, including virus particles. As different bulk solutions flow over the sensor or as particulates adsorb onto the quartz sensor, the vibration frequency of the sensor changes. These changes in the frequency are measured by the QCM-D (Biolin Scientific, 2014). The quartz crystal sensors can be coated by a variety of materials, such as silica to mimic sand surfaces. This process is summarized in the figures below using a solution containing MS2 virus particles as an example.

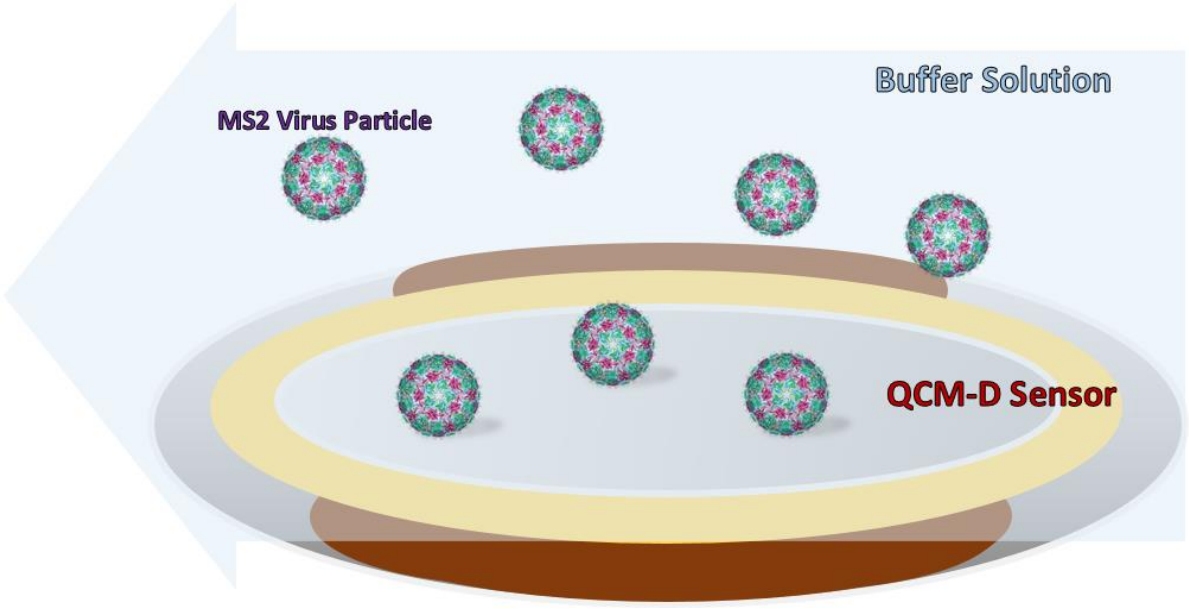

Figure 5: A buffer solution containing MS2 virus particles flows through the QCM-D chamber and over the quartz crystal sensor. Some of these particles adsorb to the surface of the sensor.

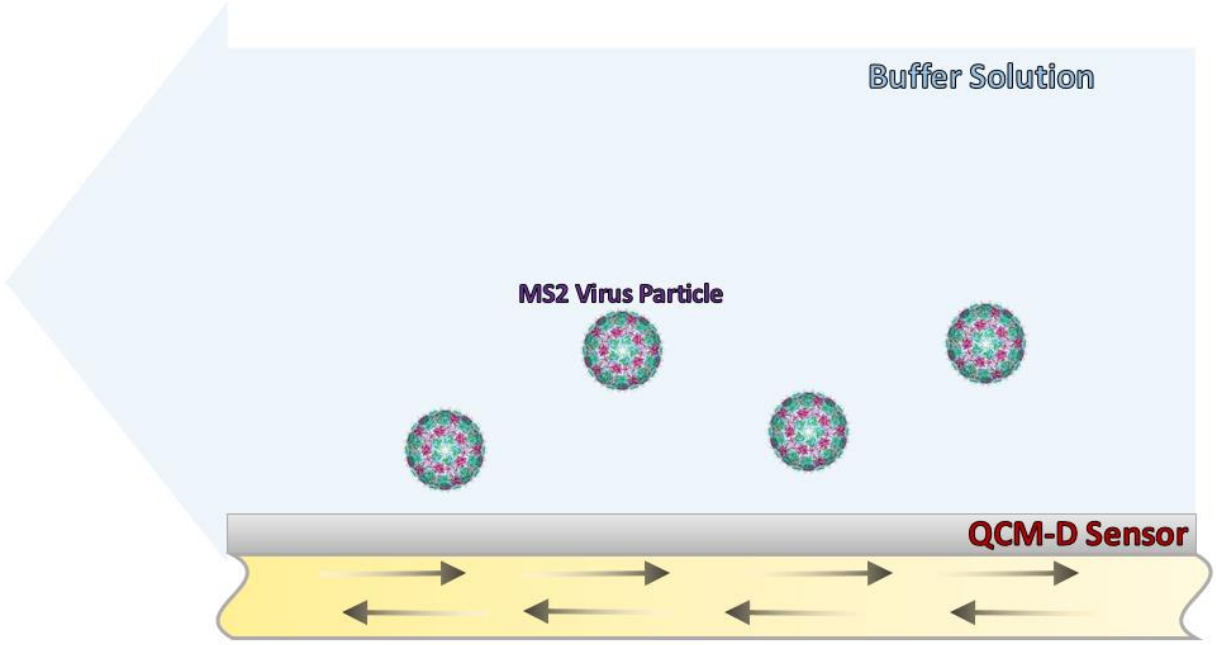

Figure 6: The quartz crystal sensor vibrates at a certain frequency when an electric current is applied to it.

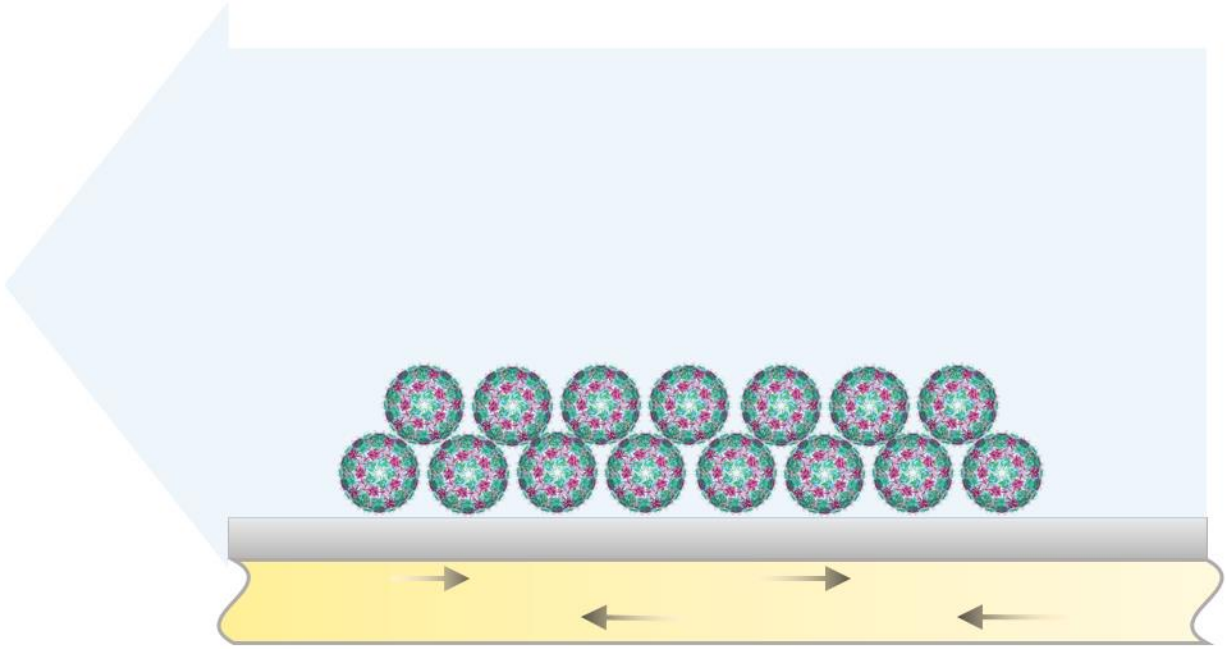

Figure 7: Once the MS2 virus particles adsorb onto the sensor, it dampens the frequency of the sensor.

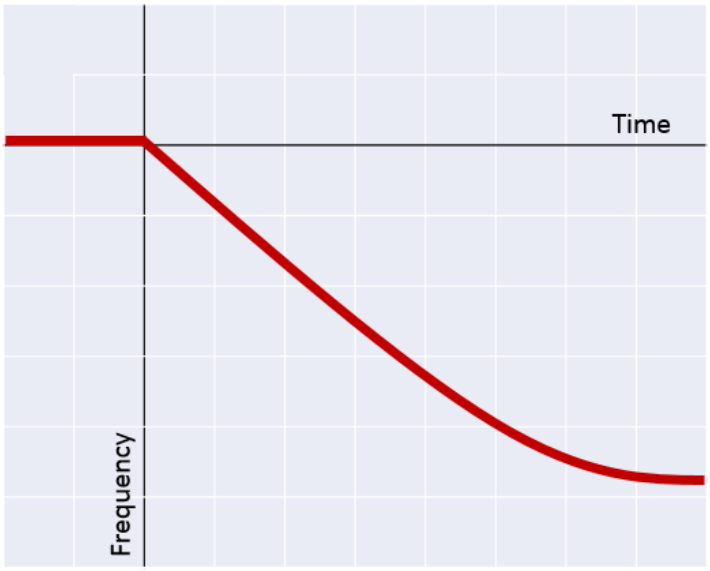

Figure 8: The dampening of the sensor's vibration is measured by the QCM-D instrument as a decrease in frequency over time. *Typically, the frequency decreases at a constant rate before eventually leveling out once the sensor becomes saturated with the virus particles. The initial, relatively constant rate of frequency change, can be used to qualitatively compare the deposition rates of different test solutions.*

Experiments with the QCM-D can be customized to simulate the natural conditions to study the behavior of viruses in the environment. As mentioned earlier, the quartz sensors can be coated to mimic a soil surface. The solution that flows over the quartz sensor can be designed to model the chemistry of natural waters in pH, ionic strength, and buffer composition. Unlike other methods of studying viral deposition behavior such as columns, major benefits of the QCM-D include the ability to precisely control the surface properties of the silica surface. The QCM-D sensor allows for much greater precision compared to packed granular material, measuring the actual changes in mass accumulating on the absorbent surface (Biolin Scientific, 2014). The high sensitivity is an important requirement when dealing with viruses like MS2 which are very small (26 nm in diameter) and experience minimal deposition due to strong negative charges. The

changes in frequency gathered can be used to compare deposition rates both qualitatively (change in frequency over change in time) or quantitatively through the use of modelling.

1.6 Related Research with QCM-D and MS2

A few studies have researched viral transport behavior through groundwater by using the QCM-D and MS2. Yuan et al., researched the deposition behavior of MS2 particles on silica sensors in the presence and absence of natural organic matter (2008). The study also examined the effects of different buffers (phosphate buffer and bicarbonate buffer) and varying ionic strength on MS2 deposition. In phosphate buffer, hydrodynamic diameter measurements suggested that the MS2 particles had aggregated, proposing that the most likely cause was the positively charged lysine on the outside of the capsid structure. When bicarbonate was used as the buffer, aggregation did not take place. The rate of MS2 deposition on the silica sensor increased as ionic strength increased, peaking at about 0.8 Hz/min at 100 mM ionic strength. These tests were conducted at pH 6, a temperature of 25 °C, an MS2 concentration of 10^{10} plaque forming units per milliliter (PFU/mL), and a buffer concentration of 1 mM $NaHCO_3$. The study also found that deposition rates decreased when ionic strength increased above 100 mM.

Tong et al. also researched the deposition behavior of MS2 particles on silica sensors using QCM-D (2012). The team conducted tests to assess how solution pH, ionic strength, and buffer chemistry affect MS2 deposition onto silica sensors. Tong et al. quantified deposition using deposition efficiency, calculated as the ratio of the deposition rate on silica to the favorable deposition rate on poly-l-lysine (PLL) hydrobromide coated silica sensors (non-repulsive) with the same test conditions. Using test solutions containing an MS2 concentration of 2×10^{8} PFU/mL and at pH values of both 6 and 9, they found that MS2 deposition efficiency increased

as ionic strength increased. This trend remained true using buffer solutions of NaCl, $CaCl_2$, and $MgCl_2$. These observations are in agreement with the results found by Yuan et al. This study also found that MS2 deposition efficiency was generally greater at pH of 6 compared to pH 9 while keeping ionic strength and buffer chemistry constant. This is most likely because the capsid protein is more negatively charged at higher pH, thus increasing the repulsive electrostatic force between the MS2 particle and the negatively charged silica surface. Using the divalent buffer solutions, $CaCl_2$ and $MgCl_2$, also resulted in higher deposition efficiencies compared to the monovalent NaCl solution. These results were in agreement with DLVO theory.

A major issue with using the QCM-D to study deposition behavior is that any material in the stock solution that is not the targeted virus also has the potential to deposit onto the sensor, and there is no way to distinguish the deposition of the target virus from other material. For this reason, the purity of the virus stock solution is imperative to accurate QCM-D data. In both studies described above, the purification process used can be greatly improved upon. The method of purifying MS2 stock solutions used by Yuan et al. and Tong et al. utilized sequential filtering. MS2 virus was inoculated into a broth containing *E. coli* cells and allowed to replicate. This solution was then initially purified by adding Polyethylene glycol and NaCl to the solution and centrifuging to separate the MS2 virus from the *E. coli*. This MS2 containing supernatant was then resuspended and then filtered through a 0.2 µm polycarbonate low protein binding membrane in a microfiltration vacuum unit. The MS2 stock solution was then concentrated and stored. As a result of this purification approach, the final stock solution contains all of the material in the *E. coli* and MS2 mixture that is less than 0.2 µm. It is thus expected that the deposition they observed contained a mixture of different proteins, lipids, as well as the MS2 particles. Tong and Yuan's MS2 purification process for the MS2 virus stock can be vastly

improved upon to better guarantee the absence of potentially interfering material and the accuracy of the QCM-D tests.

1.7 Study Objectives

Viruses can be exposed to oxidative stress via naturally occurring sources or through water treatment. The oxidation of virus structural components may impact viral transport through the subsurface in groundwater. This potential impact can be explored by studying the deposition behavior of MS2 particles that have briefly reacted with free chlorine, causing limited inactivation. Using QCM-D technology, the impact of oxidation on virus deposition in simulated groundwater conditions can be explored with a greater level of precision than what is capable with other experimental methods. Overall, this study has three objectives: 1) optimize measured values of MS2 deposition by ensuring highly pure MS2 virus stock and adjusting solution chemistry, 2) determine any change in the deposition rate of MS2 particles after oxidation with free chlorine, and 3) explain any changes in the observed deposition behavior based on previous knowledge of MS2 protein structure and reactions in the virus proteins.

Chapter 2: Materials and Methods

2.1 Chemicals

All chemicals were used as received and water used in the experiments was purified by a Hydro Analyzer Water System (AWS 200).

The following chemicals and biological products were purchased from Fisher Scientific Inc. (Waltham, MA): Sodium bicarbonate ($NaHCO_3$), potassium nitrate (KNO_3), hydrochloric acid (HCl), sodium phosphate potassium heptahydrate ($Na_2HPO_2 \bullet 7H_2O$), sodium chloride

(NaCl), sodium phosphate monobasic monohydrate ($NaH_2PO_4 \cdot H_2O$), and bovine serum albumin (BSA). The following additional chemicals were purchased from Acros (New Jersey, USA): Sodium thiosulfate pentahydrate ($Na_2O_3S_2 \cdot 5H_2O$), N,N-Diethyl-p-phenylenediamine sulfate ($(C_2H_5)2NC_6H_4NH_2 \cdot H_2SO_4$), calcium chloride ($CaCl_2$), sodium hypochlorite (NaClO), chloroform ($CHCl_3$), and streptomycin sulfate ($C_{42}H_{78}O_{24} \cdot 3H_2SO_4$). Potassium permanganate ($KMnO_4$) were purchased from Alfa Aesar (Royston, Hertfordshire, England). Sodium dodecyl sulfate ($NaC_{12}H_{25}SO_4$), ethylenediaminetetraacetic acid disodium salt dehydrate ($C_{10}H_{14}N_2Na_2O_8 \cdot 2H_20$), and Polyethylene glycol (PEG) ($H(OCH_2CH_2)nOH$ were purchased from Sigma-Aldrich (St. Louis, MO). D-glucose ($C_6H_{12}O_6$) and potassium phosphate monobasic anhydrous (KH_2PO_4) were purchased from Amresco Inc. (Solon, OH). Sulfuric acid (H_2SO_4) was purchased from VWR International (Radnor Township, PA). Sodium hydroxide (NaOH) was purchased from J.T. Baker (Center Valley, PA). Bacto tryptone, Bacto yeast extract, and Bacto agar were purchased from Becton, Dickinson and Company (East Rutherford, NJ). Compressed nitrogen gas (N_2) was purchased from Airgas (Radnor Township, PA). Hellmanex III was purchased from Hellma GmbH & Co. KG (Mülheim, Germany).

2.2 Methods

2.2.1 Purification of MS2 (Eric's and Krista's)

Bacteriophage MS2 (ATCC® 15597-B1™) was propagated via infection of host *Escherichia coli* (ATCC® 15597™) and later purified and concentrated as described in Pecson et al. (2009). Initially, 5 mL of *E. coli* was inoculated into 1 liter of LB broth (composed of 10 g Bactotryptone, 1 g of yeast extract, and 8 g of NaCl; supplemented with 0.3 g of $CaCl_2$, and 2 mg of streptomycin sulfate) and allowed to reach log phase at roughly 10^7 colony forming unit per

milliliter (CFU/mL). The solution was then inoculated at a multiplicity of infection of 0.1 with 10 µL of an MS2 virus stock with a concentration of approximately 10^{11} PFU/mL and allowed to incubate for five hours. Afterwards, 5 mL of chloroform was mixed with the liter of bacterial-viral solution to lyse the bacteria. The suspension was then centrifuged for 15 min at 4,000 × g to pellet out the bacterial debris and separate it from the suspended MS2 virus particles. The resulting 1 liter of supernatant containing the MS2 virus was stored overnight at 4 °C with 10% PEG (PEG 6000; Sigma Aldrich) and 0.5 M NaCl. The PEG containing solution was later centrifuged at 7,000 × g for 45 min, creating a pellet containing the MS2 virus. The pellet was resuspended over 2 hours with about 40 mL of phosphate buffer (5 mM NaH_2PO_4, 10 mM NaCl, pH 7.4). The PEG was then pelleted by centrifugation at 10,000 × g for 10 minutes and the supernatant containing the MS2 virus was collected. 10 mL of chloroform was added to the 40 mL and mixed into the solution to remove the remaining PEG. The solution was centrifuged for 10 min at 3,000 × g to separate the remaining PEG from the rest of the solution. The process of adding chloroform and centrifuging was repeated two to three times. The solution was transferred to a new tube, and compressed air was bubbled through the liquid to volatilize any remaining chloroform. The solution was concentrated in an Amicon centrifugal filter with a 100 kDa cut-off (Millipore, Billerica, MA), washed ten time with phosphate buffer in the same filter, and then passed through a 0.1 µm pore polyvinylidene difluoride filter (Millipore, Billerica, MA). The resulting MS2 virus stock solution was purified further with fast protein liquid chromatography (FPLC). In brief, FPLC was conducted in a Biorad Econo system with a GE Healthcare HiPrep 26/60 Sephacryl S-400 HR Column. The virus peak was concentrated with a Millipore Centricon 100 and then further purified by passing the virus concentrate through a 0.1 um pore nitrocellulose cartridge filter. The final stock solution went through a buffer exchange to

suspend the MS2 virus in the desired buffer for QCM-D analysis. The concentration of infective MS2 viruses was quantified using a double-layer agar technique (American Public Health Association, American Water Works Association, Water Environment Federation, 2005), and measured as PFU/mL. The final stock was concentrated to be no less than 2×10^{12} PFU/mL. This minimum stock concentration was necessary to retain a sufficiently concentrated virus solution after mixing with the free chlorine mixture. The volume of the MS2 spike into the free chlorine solution was always less than 10% of the final test solution volume.

The double-layer plaque assay involves cultivating *E. coli* with MS2 viruses on a plate containing a layer of hard agar covered by a layer of soft agar. The hard agar base contains 7.5 g/L agar and growth media. The growth media contains 5.0 g/L Bacto trypton, 0.5 g/L yeast, and 4.0 g/L sodium chloride and is supplemented with a $CaCl_2$ solution (10.0 g/L D-Glucose, 3.0 g/L $CaCl_2$), and streptomycin sulfate solution (40 mg/L streptomycin). The overlaying soft agar contains 2.5 g/L agar and growth media. The soft agar is stored in a tube and is melted at 95 °C prior to MS2 plating. For plating, 100 µL of *E. coli* and 100 µL of the MS2 sample are added to the tube with the melted soft agar and then poured on top of the hard agar layer in the plate. The agar mixture is allowed to solidify, and then incubated overnight at 37 °C. The MS2 viruses form plaques in the *E. coli* "lawn" due to host infection. The plaques are counted the following day, and the concentration of infective MS2 viruses in the original stock is determined based on the serial dilution of the plated sample.

2.2.2 Free Chlorine Buffer Solution Preparation

The buffer solution was optimized in order to allow for optimal measurable deposition by the QCM-D, maintain a specific pH through the procedure, mimic a natural environment, and avoid impurities that would interfere with accurate QCM-D data collection.

The optimized buffer solution was prepared with a pH of 5 in order to encourage the deposition of MS2 particles while not risking virus inactivation at low pH values. A phosphate buffer was selected over a carbonate buffer to minimize changes in pH from equilibrating with the air in the open test environment. The ionic strength was adjusted to 100 mM to encourage deposition as reported by Yuan et al and Tong et al. This also assists in avoiding major shifts of ionic strength by pH adjustment and the addition of virus stock. Potassium nitrate was selected to obtain the ionic strength because of its high purity compared to other inert salts. Free chlorine was added as sodium hypochlorite.

The free chlorine buffer solution was composed of 15 mM phosphate and 77.5 mM potassium nitrate, and prepared in 1 liter stocks. The solution was adjusted to pH 5 with HCl and NaOH. The solution was then autoclaved to eliminate any microorganisms. After cooling, the solution was filtered through a 0.22 µm sterile filter to remove any particulate matter that would interfere with measuring MS2 deposition with the QCM-D. The pH of the buffer was then checked under sterile conditions to confirm that it remained at pH 5. A small volume of sodium hypochlorite was then added to the buffer solution until the desired concentration of free chlorine was reached, as measured by the standardized DPD (N,N-diethyl-p-phenylenediamine) colorimetric method (Standard Methods for the Examination of Water and Wastewater, 14th Ed., 1975). The stock free chlorine buffer solution was stored at 4 ^{0}C and used within one month of preparation.

2.2.3 Chlorine Demand

The chlorine demand of the MS2 test solutions were measured to determine an optimal MS2 and chlorine concentrations. 2 mL of the free chlorine buffer solution was poured into a chlorine-demand-free glass tube (i.e., presoaked in a 10% bleach bath for at least 24 hours). The free chlorine buffer solution was then spiked with MS2 to reach a concentration of $4x10^{11}$ PFU/mL and mixed via vortex for a predetermined contact time. Per the standardized DPD (N,N-diethyl-p-phenylenediamine) colorimetric method, the MS2 test solution was then quenched with the DPD solution. The solution absorbance at 515 nm was measured with a spectrophotometer and the chlorine concentration was determined from a calibration curve. The chlorine demand of the MS2 test solution was determined by plotting the measured absorbance against contact time.

2.2.4 Controlling Extent of Reaction Inactivation Measurements

The extent of the reaction between the MS2 virus and free chlorine was controlled and measured as the product of the initial free chlorine concentration and contact time (concentration × time, units mg/L × sec). To assess damage to the MS2 virus caused by exposure to free chlorine, the amount of virus inactivation in each test was measured. The free chlorine buffer solution was poured into a chlorine-demand-free glass tube that was submerged in a 10% bleach bath for at least 24 hours. The buffer was spiked with a specific amount of the virus stock so that the final solution had an initial infective MS2 concentration of $4x10^{11}$ PFU/mL and a total volume of 2 mL. The solution was then mixed via vortex for the predetermined amount of contact time. The chlorine reaction was quenched at the desired contact time using a 0.21 mM sodium thiosulfate solution, roughly 5 times the molar concentration necessary to fully quench

the chlorine. The remaining infective MS2 concentration and the subsequent $\log_{10}$ inactivation was determined by the double-layer agar technique. This final MS2 test solution was pumped through the QCM-D instrument to measure the adsorption of MS2 particles onto the silica sensor after reacting with free chlorine.

2.2.5 Quartz Crystal Microbalance with Dissipation Procedure

The QCM-D E4 system consists of 5MHz AT-cut quartz crystal sensors, flow chamber modules, a peristaltic pump, and Teflon tubes. Test solutions are pumped by the peristaltic pump at a slow enough rate to ensure laminar flow through the tubes and into the flow chamber module. Sensors are housed in the flow chamber module and test solutions are pumped over the sensor. Particles present in the test solution interact with and deposit onto the sensor, changing the sensor vibration frequency. The deposition rate of the particles in the test solution is recorded by measuring the change in vibration frequency over time.

Quartz crystal sensors are initially plated with gold. Sensors can also be prepared with a number of other surfaces, such as silica or various polymers. For most of the research presented here, sensors with a silica coat were employed to model a sand particle surface that a virus particle would interact with as it travels through the subsurface or in a sand filtration unit.

Cleaning Procedure

Sensors

Prior to use, the silica-coated sensors were soaked in 2% SDS solution overnight to loosen any material that might be adhered to the surface. The silica sensors were then rinsed thoroughly with DI water and dried with inert ultrahigh-purity nitrogen gas. Afterwards, the silica sensors were oxidized in a UV chamber for 30 minutes to disinfect any microorganisms on

the surface. Finally, any remaining debris was removed using the inert ultrahigh-pure nitrogen gas before being placed in the QCM-D chamber.

Repeated cycles of this cleaning process and the transfer of the sensors to and from the QCM-D chamber would eventually result in chips and scratches on the sensors. Sensors were discarded once significant chipping or scratching appeared, or after they had been used for a total of five tests. Sensors that were used beyond five tests typically had erratic frequency readings, making it difficult to establish the baseline and collect accurate data.

Chamber

A deep thorough cleaning of the flow module chambers occurred once a month to remove any material that might have deposited on the inside of the chamber. The chamber was soaked in 2% SDS solution, heated to ~40 ^{0}C, and sonicated for 10 minutes. The chamber was then thoroughly rinsed with DI water and dried with ultrahigh-pure nitrogen gas. The rubber O-ring and stopper would also be replaced regularly once a month.

Teflon Tubes

At the beginning of each day of tests, any residual debris or microbial growth that might have occurred overnight was removed from the Teflon tubes by pumping through 2% Hellemax III with the pump set at its highest speed for 10 minutes (0.579 mL/min). To rinse afterwards, DI water was pumped through the Teflon tubes at the highest speed for 10 minutes. After each test, the Teflon tubes were cleaned by pumping through 2% SDS solution with the pump set at its highest speed for 10 minutes and then rinsed with DI water for 10 minutes. The Teflon tubes were regularly replaced after 3 months of use.

Experimental Procedure

Cleaned silica sensors were mounted in the QCM-D flow chamber modules. The QCM-D flow chamber modules were then set to maintain a temperature of 25 ^{0}C. The instrument first finds the resonance frequency of the 3rd, 5th, 7th, and 9th harmonics of the sensor (f3, f5, f7, and f9). Before each test, the sensor was equilibrated by pumping quenched chlorine buffer solution through the chamber at 0.1 mL/min until the recorded frequency remained steady, changing less than 1 Hz over 30 minutes. After the baseline was established, the pump was turned off, and the receiving end of the Teflon tube was placed in the test solution. Care was taken to avoid the introduction of air bubbles into the tube. The test solution was then pumped through the chamber and over the sensor at 0.1 mL/min. Once the test solution reached the sensor, deposition was observed and measured by the decreasing frequency of the sensor on the 3rd, 5th, 7th, and 9th harmonic. The pump was left on until the entire solution was pumped through.

Data Analysis

Data was collected using QSoft software. The changing frequency of the quartz crystal sensor over time was measured on four different harmonics (f3, f5, f7, and f9), with a data point taken every 0.6 seconds for each ~20 minute test. The data collected for the four harmonics was then plotted as frequency (Hz) versus time (seconds). The four harmonics create very similar shaped plots, but only the frequency change over time for f3 was used to represent the MS2 deposition rate for comparing data sets and identifying trends, consistent with the studies conducted by Yuan et al. and Tong et al. However, because of the occasionally erratic nature of the QCM-D, the general shape of the change in f3 was compared to the other harmonics. If the shape of f3 diverged away from the other harmonics, the test was deemed erroneous and

discarded. Poor tests could have been a result of any number of factors including a worn out sensor, a chamber requiring cleaning, or excessive air in the test solution. Test results were also discarded if baseline could not be established between -1.5 Hz/hr and 1.5 Hz/hr. Values below this range suggest deposition of particulates onto the sensor, and values above this range suggest the removal of material from the quartz crystal sensor. Both conditions signify either an erroneous reading or a damaged sensor.

To normalize the results, the initial change in frequency was calculated as the difference between the recorded initial change in frequency minus the slope of the baseline. Based on detection limits for the QCM-D, if the initial change in frequency was calculated to be less than 1.5 Hz/hr, or if the initial change in frequency lasted less than 5 minutes, it was assumed there was no deposition (Biolin Scientific, 2012).

The data collected was grouped by reaction time (units mg/L × sec) and inactivation level (units $\log_{10}$) and plotted. The Student's t-test, which determines whether two sets of test data are significantly different based on the probability that the two sets have the same population and mean, was used to compare the data groupings for each mg/L_0 × sec and $\log_{10}$ inactivation value with at least three successful tests. When calculating averages and standard deviations for plots or for use in the Student's t-test, deposition data was ignored from tests without at least two other duplicates. Deposition data was also ignored if it was an outlier compared to the other measured rates for that specific reaction time or inactivation level as determined by the extreme studentized deviate method with a confidence interval of 95%. The Student's t-test considers the size, mean, and standard deviation of the two data sets being compared.

Chapter 3: Results and Discussion

3.1 Proof of Concept: Measuring Deposition of Oxidized Bovine Serum Albumin Protein

Before attempting tests with MS2 virus, tests were conducted using bovine serum albumin protein (BSA) in lieu of MS2 virus to explore if a protein's deposition behavior would change after reacting with free chlorine. BSA is a convenient surrogate because it is easily purchased with high purity and is a commonly used protein for deposition demonstrations with the QCM-D instrument. The structure of BSA unfortunately does not match the complexity of the MS2 protein capsid structure. However, it was assumed that it would be adequate in determining if the presence of an oxidative stress would change the deposition rate of a protein.

The chlorine demand of a BSA solution was first determined to identify an adequate BSA concentration and free chlorine dose. Tests began with a BSA concentration 4 mg/L in a bicarbonate buffer (10 mM bicarbonate, 75 mM potassium nitrate) and 3 mg/L free chlorine. The concentration of free chlorine was measured before and after 10 seconds of reaction time. It was assumed that 10 seconds would be the greatest contact time utilized on MS2 test solutions before excessive inactivation would occur. As displayed in Table 3, after three tests, it appeared that the chlorine demand of the 4 mg/L of BSA was less than 10% of the initial free chlorine concentration. This was ideal for analytical purposes as it could be assumed that the reaction followed 1st order kinetics.

Test #	*$[Cl_2]_0$, mg/L*	*$[Cl_2]$, mg/L*	*Cl_2 Demand, mg/L*	*% Drop*
1	2.81	2.56	0.25	8.17
2	2.75	2.44	0.31	10.13
3	2.81	2.56	0.25	8.17
Average				8.82

Table 3: Chlorine demand of 4 mg/L BSA, showing the difference in initial and final measured free chlorine.

The deposition rate of BSA onto silica sensors was measured without reacting with free chlorine to determine if the concentration of BSA was adequate for the deposition to be detectable by the QCM-D instrument. As shown in Figure 9, a total of seven tests were conducted with a BSA concentration of 4 mg/L. Measured values ranged from 0 Hz/hr to 2.16 Hz/hr with an average of 0.60 Hz/hr. With all measured values being below the minimum threshold of the QCM-D instrument, it was concluded that there was no measurable deposition.

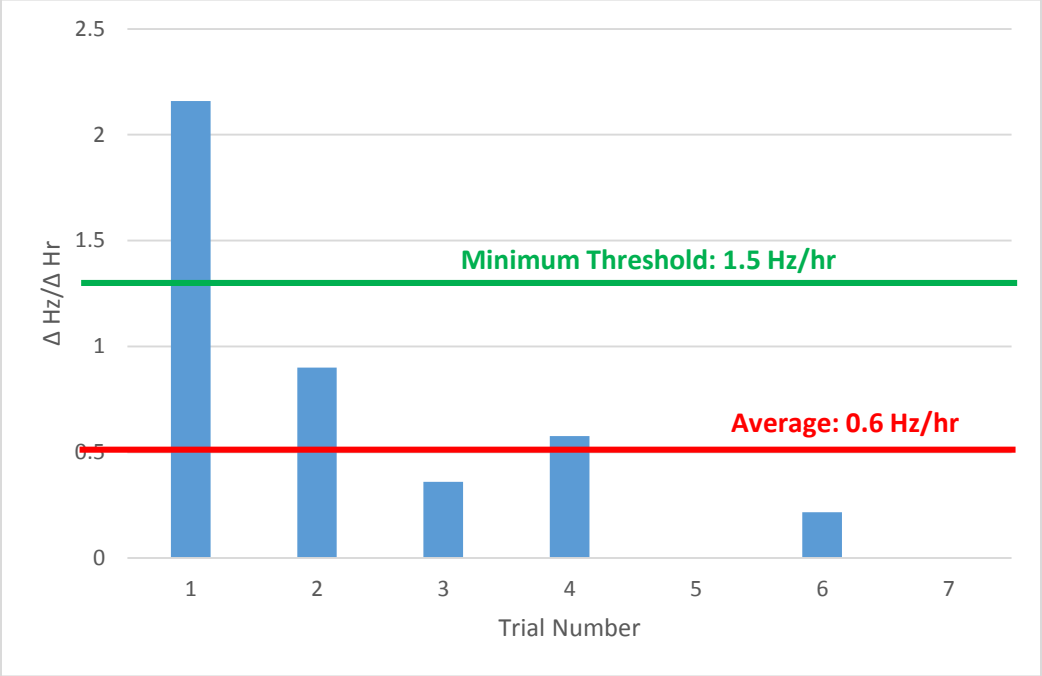

Figure 9: Measured deposition rates of 4 mg/L BSA.

To increase detectability, the BSA concentration was increased to 40 mg/L, closer to the 50 mg/L is used for QCM-D demonstrations with BSA (Biolin Scientific, 2012). Although this likely increased the chlorine demand, it was decided that retaining first-order kinetics was not necessary to determine if free chlorine changed the BSA protein deposition behavior. While dosing at 3 mg/L free chlorine, the QCM-D was able to have a consistent reading of the BSA deposition at contact times of 0, 5, and 10 seconds. An example QCM-D reading of the BSA deposition is shown in Figure 10.

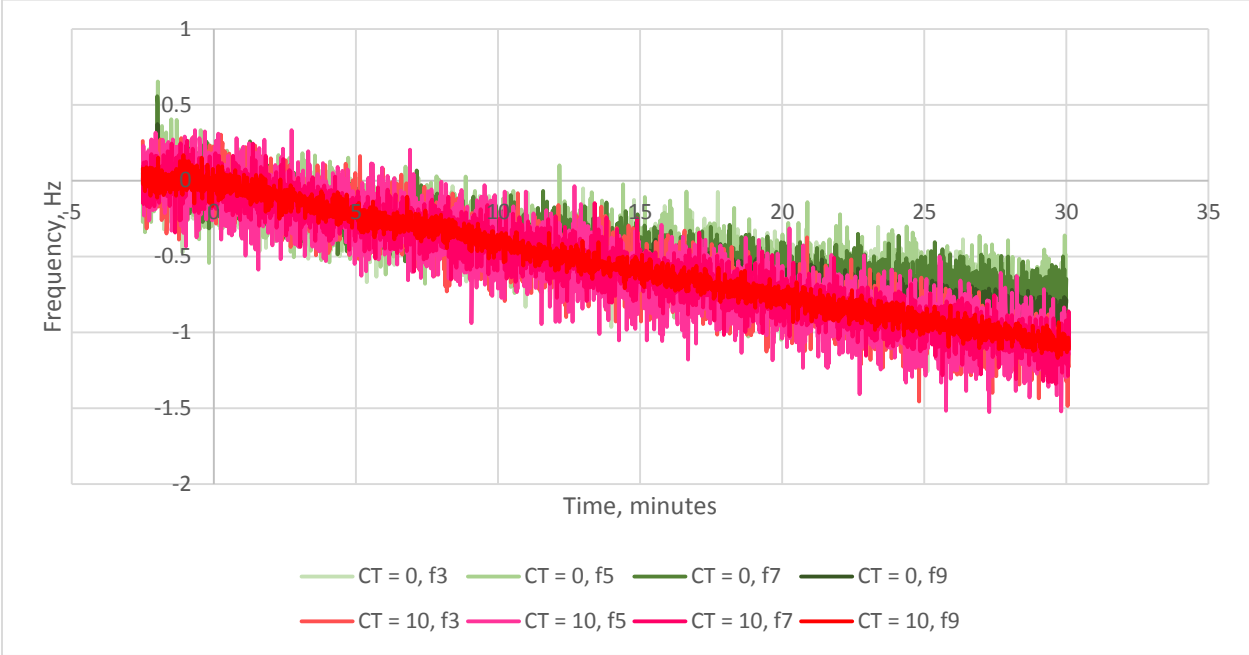

Figure 10: Example plot of the change in frequency (Hz) versus the change in time (minutes) for the 3rd, 5th, 7th, and 9th harmonics for 40 mg/L BSA with a CT value of 0 (green) and a CT value of 10 (red). *The frequency of the BSA test solution reacted with free chlorine decreases at a faster rate, indicating deposition at a faster rate.*

Eight trials were conducted for each contact time. Even though readings from the QCM-D were consistent for each amount of contact time, the data collected remained under the 1.5 Hz/hr threshold. However, the data as shown in Figure 11 did suggest an increased rate of deposition for BSA that reacted with free chlorine compared to BSA that did not react with free chlorine.

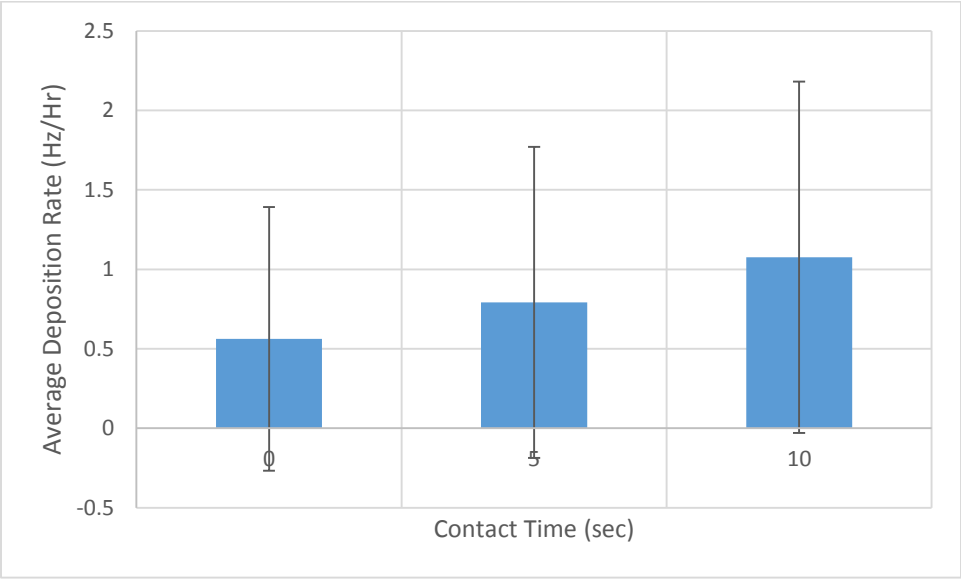

Figure 11: Contact time versus average deposition of 40 mg/L BSA. *Error bars show 95% confidence for t-distribution.*

Using the 2-tailed Student's t-test, there was a low calculated probability that there was a difference between the deposition rate of BSA that reacted with free chlorine for 0 seconds and 5 seconds (roughly only 50% likelihood they are statistically different). However, also using the 2-tailed Student's t-test, the calculated probability that there was a difference between the deposition rate of BSA that reacted with free chlorine for 5 seconds and 10 seconds was 94.5%. Finally, the calculated probability that there was a difference between the deposition rate of BSA that reacted with free chlorine for 0 seconds and 10 seconds was 97.3%. These results, as summarized in Table 4, suggested that BSA protein that reacted with free chlorine does exhibit different deposition behavior, leading to the hypothesis that a similar change could be measured with MS2 particles.

Contact Time (sec)	0	5	10
0		49.7%	97.2%
5	49.7%		94.5%
10	97.2%	94.5%	

Table 4: Comparison of data sets for different free chlorine contact times with BSA using Student's t-test (2-tails). *Percentages shown are the probability the two data sets are statistically significantly different. A 95.0% chance of a difference was assumed to be significant. Significant differences between deposition rates were highlighted in green. Insignificant differences were highlighted in red.*

3.2 Procedure Optimization: Virus Stock Purity

The impact of virus purity on deposition experiments was investigated. Three tests were conducted to measure the deposition rate of the MS2 particles before utilizing the FPLC purification process. These tests included contact times of 0 and 10 seconds with 3 mg/L free chlorine, as well as ionic strengths of 10 mM and 100 mM, pH values of 6 and 7, and temperatures of 20 ^{0}C and 25 ^{0}C. All tests used an MS2 concentration of 10^{11} PFU/mL and a 5 mM bicarbonate buffer.

Deposition rates without FPLC purification consistently measured above the QCM-D threshold of 1.5 Hz/hr. Deposition rates also appeared to be significantly higher when contact time with free chlorine increased to 10 seconds. Following this, an MS2 virus stock was purified using the FPLC process. Two tests were conducted with this FPLC purified stock, both at a pH of 6 and ionic strength of 100 mM. Both had CT values of 0 mg/L × sec, and used an MS2

concentration of 10^{11} PFU/mL. Deposition rates measured during these trials were significantly less than what was measured before utilizing FPLC. Both trials failed to measure a significant deposition rate above the QCM-D threshold of 1.5 Hz/hr. These results, summarized in Table 5, suggested that deposition rates measured without the FPLC purification step are likely influenced by background substances in the solution other than MS2 virus. As mentioned earlier, Yuan et al. and Tong et al. both employed MS2 purification processes that could be vastly improved upon. Yuan et al. measured a deposition rate of roughly 0.8 Hz/min (~50 Hz/hr) for 10^{10} PFU/mL MS2 depositing onto a silica sensor at 25 ^{0}C, pH 6, and 100 mM ionic strength in a 1 mM $NaHCO_3$ buffer. This value is much greater than what was measured in these trials, potential evidence that background substances interfere with accurate MS2 deposition readings if not removed with a thorough purification procedure. To ensure only deposition of MS2 virus was observed, all future trials were conducted utilizing MS2 virus stocks purified with the FPLC process.

Without FPLC Purification					With FPLC Purification				
Test #	**IS (mM)**	**pH**	**CT (sec)**	**Dep., Hz/hr**	**Test #**	**IS (mM)**	**pH**	**CT (sec)**	**Dep., Hz/hr**
7	10	7	0	2.16	19	100	6	0	0.47
8	10	7	10	9.58	22	100	6	0	0.72
10	100	7	10	23.76					
			Average	**11.83**				**Average**	**0.59**

Table 5: Differences between measured deposition rates of 1x10^{11} PFU/mL MS2 virus solution purified with and without FPLC. *The 5th harmonic (f5) was used to represent the deposition rate for these tests in order to include the data from test #22. The shape f3 diverged away from the other harmonics in test #22. Deposition values greater than 1.5 Hz/hr were considered to be measurable MS2 deposition (highlighted in green). Deposition values less than 1.5 Hz/hr (highlighted in red) were not considered to be measurable MS2 deposition.*

3.3 Procedure Optimization: Buffer Solution

As understood from electrostatic forces, an acidic buffer solution was prepared with a high ionic strength to enhance deposition. As explained in the methods section, a phosphate buffer minimized the pH changes observed when a bicarbonate buffer was employed, particularly in procedure steps that were conducted in the open air. Bicarbonate and phosphate buffers were also examined to see which buffer allowed for more consistent and measurable deposition. Two tests were conducted to measure the deposition rate of MS2 particles in a 5 mM bicarbonate buffer. Both tests were conducted with a solution at a pH of 6, ionic strength of 100 mM, no contact time with free chlorine, a temperature of 25 ^{0}C, and an MS2 concentration of 10^{11} PFU/mL. Measured deposition rates using the bicarbonate buffer were both below the QCM-D threshold of 1.5 Hz/hr. Following this, four tests were conducted with a 15 mM phosphate buffer. Trials were conducted at both pH 5 and 6, an ionic strength of 100, no contact

time with free chlorine, a temperature of 25 ^{0}C, and an MS2 concentration of 10^{11} PFU/mL. Deposition rates measured during these trials were significantly higher than those with the bicarbonate buffer. Most tests were above the QCM-D threshold of 1.5 Hz/hr. These results, as summarized in Table 6, suggest that phosphate buffer improves MS2 deposition onto the silica sensor into measureable levels. Consequently, phosphate buffer was used for all future trials.

5 mM Bicarbonate Buffer			**15 mM Phosphate Buffer**		
Test #	**pH**	**Dep., Hz/hr**	**Test #**	**pH**	**Dep., Hz/hr**
19	6	0.47	24	5	1.44
22	6	0.72	27	5	1.94
			30	5	3.31
			48	6	2.34
Average		**0.59**	**Average**		**2.26**

Table 6: Differences between measured deposition rates of 1x10^{11} PFU/mL MS2 in 5 mM bicarbonate buffer and 15 mM phosphate buffer. *The 5th harmonic (f5) was used to represent the deposition rate for these tests in order to include the data from test #19. The shape f3 diverged away from the other harmonics in test #19. Deposition values greater than 1.5 Hz/hr were considered to be measurable MS2 deposition (highlighted in green). Deposition values less than 1.5 Hz/hr (highlighted in red) were not considered to be measurable MS2 deposition.*

Due to the large increase in MS2 deposition after switching from a bicarbonate buffer to the phosphate buffer, there was concern over the potential existence of background substances effecting the measured deposition. This was investigated by conducting tests using the 15 mM phosphate buffer with and without MS2 virus present. Three tests were considered to compare

the deposition rate of the 15 mM phosphate buffer containing 10^{11} PFU/mL MS2 with buffer containing no MS2 virus. All tests were conducted with a solution at a pH of 5, ionic strength of 100 mM, no contact time with free chlorine, and temperature of 25 ^{0}C. Measured deposition rates using the phosphate buffer were all above the QCM-D threshold of 1.5 Hz/hr. Following this, four tests were conducted with the 15 mM phosphate buffer containing no MS2 virus. Trials were conducted at pH 5, an ionic strength of 100, no contact time with free chlorine, and a temperature of 25 ^{0}C. Deposition rates measured during these trials were almost consistently below the QCM-D threshold of 1.5 Hz/hr. Only one out of the four had a measurable amount of deposition. These results, as shown in Table 7, suggest that phosphate buffer does not interfere with measured deposition, and that any measured deposition from the QCM-D can be attributed to MS2 virus.

Solution contains MS2		Solution contains NO MS2	
Test #	**Dep., Hz/hr**	**Test #**	**Dep., Hz/hr**
24	1.44	25	0.72
27	1.94	28	0.71
30	3.31	31	2.13
		32	1.08
Average	**2.23**	**Average**	**1.18**

Table 7: Differences between measured deposition rates using 15 mM phosphate buffer with and without 1x10^{11} PFU/mL MS2 to determine if the phosphate was depositing onto the silica sensor. *The 5th harmonic (f5) was used to represent the deposition rate for these tests in order to include the data from test #25. The shape f3 diverged away from the other harmonics in test #25. Deposition values greater than 1.5 Hz/hr were considered to be measurable MS2 deposition (highlighted in green). Deposition values less than 1.5 Hz/hr (highlighted in red) were not considered to be measurable MS2 deposition.*

3.4 Procedure Optimization: Free Chlorine Concentration

After establishing the necessity of FPLC purification and the optimum buffer for measurable MS2 deposition, an appropriate concentration of free chlorine was identified that both caused low inactivation levels (i.e. less than 5 $\log_{10}$ inactivation) and had contact times greater than 3 seconds, which was the practical amount of time in which an experiment could be initiated and quenched. The first conditions tested were 4 mg/L free chlorine and 4×10^{11} PFU/mL MS2. It should be noted that the MS2 concentration was increased to 4×10^{11} PFU/mL in this experiment to increase measured deposition. The chlorine demand was determined for these conditions in order to affirm first order kinetics. First order kinetics would be assumed if

free chlorine concentrations did not drop below 90% of the initial values following 15 seconds. As displayed in Figure 12, the concentration of free chlorine successfully was maintained above 90% of the original concentration.

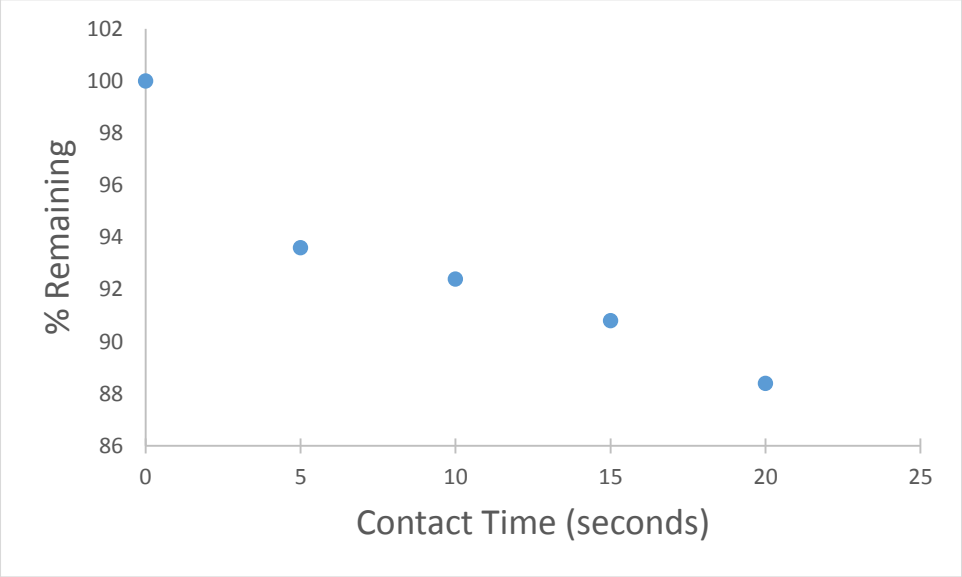

Figure 12: Chlorine demand for $4x10^{11}$ PFU/mL MS2 with initially 4 mg/L Cl_2.

However, measuring the MS2 concentration using the double layer plating method revealed that excessive inactivation occurred when using this concentration of free chlorine with this MS2 concentration. Inactivation results from the chlorine demand testing are displayed in Figure 13. Within a CT value of just 8 mg/L × sec (4 mg/L free chlorine with a contact time of 2 seconds), the MS2 test solution experienced 5 $\log_{10}$ inactivation. The target was 1-4 $\log_{10}$ inactivation to best ensure the virus structure did not begin to come apart and remain mostly intact, as suggested by Wigginton et al. (2012).

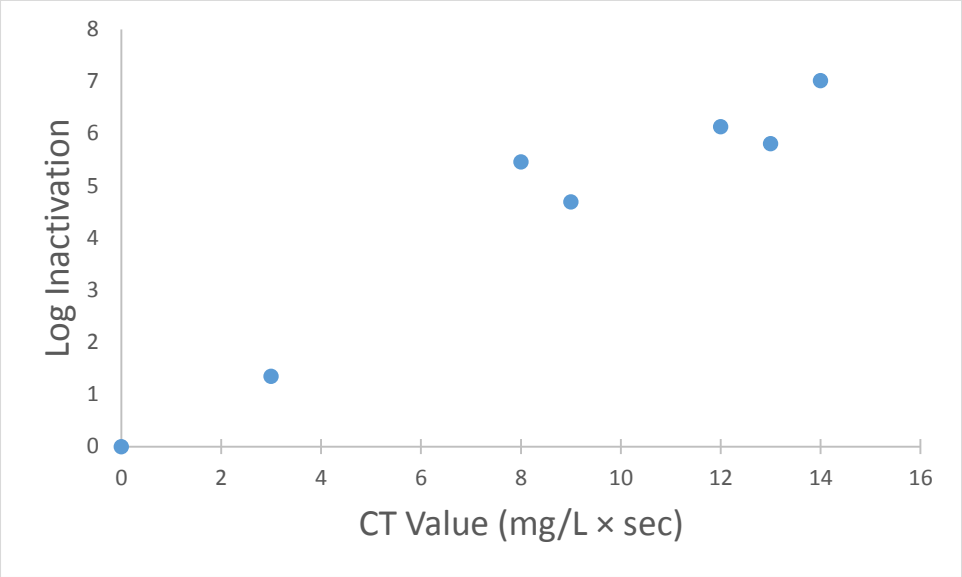

Figure 13: Log_{10} inactivation of $4x10^{11}$ PFU/mL versus CT Value.

Since it was impractical with the current methodology to decrease the reaction time below a few seconds, the concentration of free chlorine was reduced. This, however, lead to a consumption of free chlorine over 10% of the initial concentration, and therefore caused the reaction between chlorine and MS2 to deviate from first order kinetics. As a result, CT values would not be accurate means of data reporting analysis. To achieve log_{10} inactivation below 4, the concentration of free chlorine was reduced to a range of 0.3 to 3 mg/L. At this point, the optimization process was considered complete and deposition experiments commenced.

3.5 Effects of Free Chlorine Oxidation on the Deposition Kinetics of Bacteriophage MS2

3.3.1 Deposition versus Contact Time

The relationship between MS2 reaction time with free chlorine and its deposition on silica was investigated. Since first order kinetics could not be assumed, only the initial concentration of free chlorine and the reaction time were recorded for comparison. The product of the initial concentration of free chlorine ($[FC]_0$) and the reaction time (RT) was used to compare results (units mg/L_0 × sec). Deposition was calculated and expressed as Hz/hr. Data sets for product values with at least three successful tests were compared using the Student's t-test. An example QCM-D plot is shown in Figure 14.

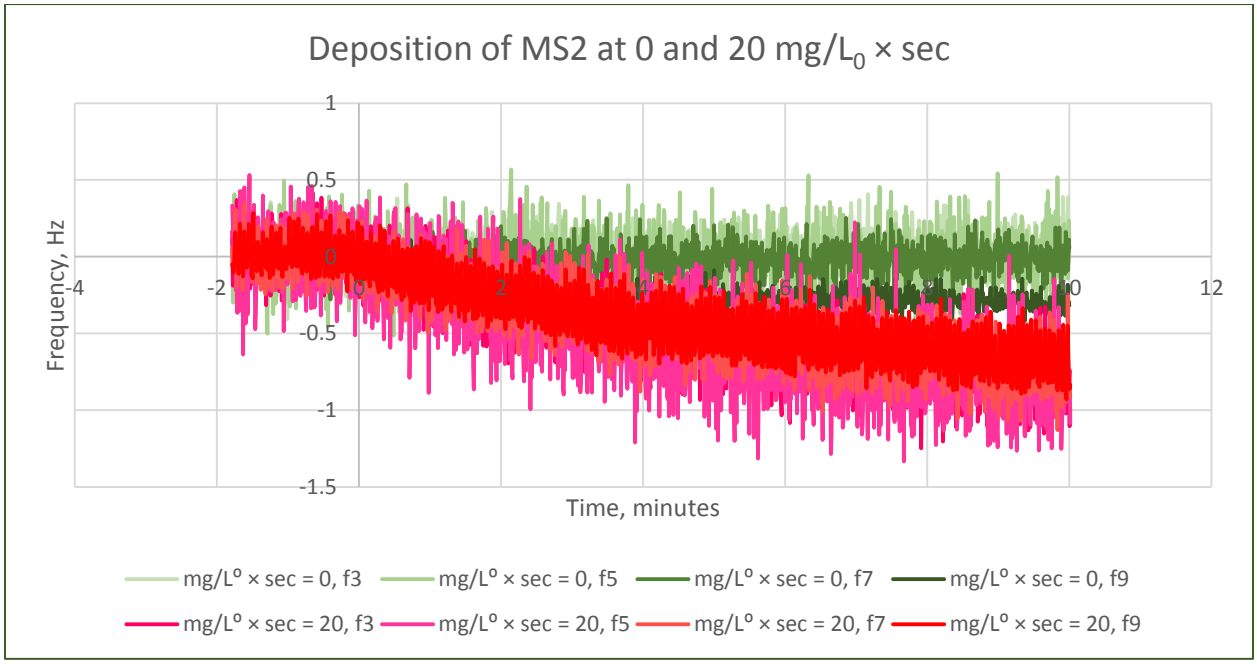

Figure 14: Example plot of the change in frequency (Hz) versus the change in time (minutes) for the 3rd, 5th, 7th, and 9th harmonics for 4x10^11 PFU/mL MS2 with a product value of 0 mg/L0 × sec (green) and a product value of 20 mg/L0 × sec (red). *The frequency of the MS2 test solution that reacted with free chlorine (red) decreased at a faster rate, indicating deposition at a faster rate compared to the MS2 test solution that did not react with free chlorine (green).*

A total of 38 tests were conducted, but 6 tests were discarded after being deemed erroneous. Figure 15 below shows all of the collected data.

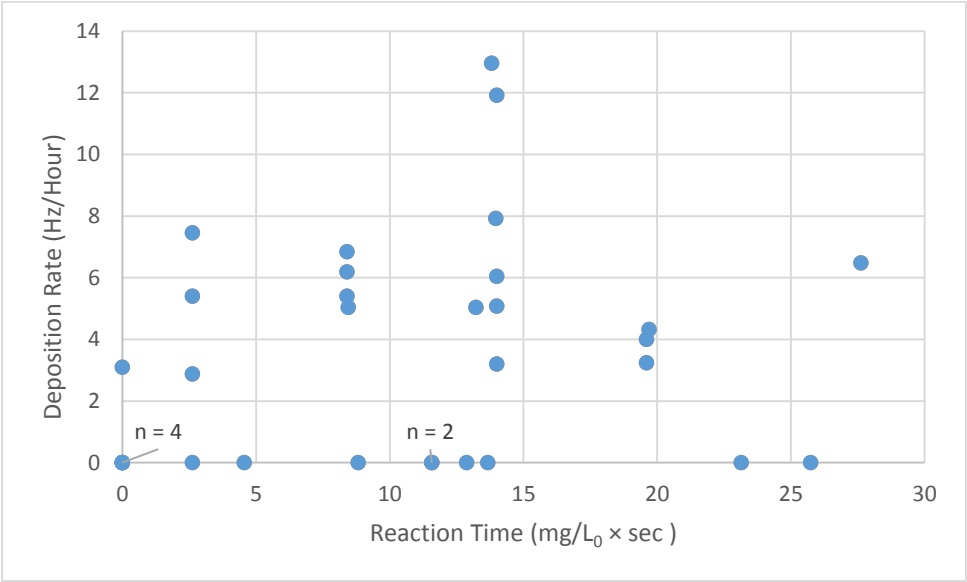

Figure 15: Plot comparing MS2 deposition rates for different RT × $[FC]_0$ values.

Based on the collected observations, deposition rates for MS2 test solutions that have reacted with free chlorine had greater deposition rates than MS2 test solutions that did not react with free chlorine. The five successful tests of MS2 test solutions that did not react with free chlorine all measured no deposition. Once the MS2 test solution reacted with free chlorine even at the smallest measured RT × $[FC]_0$ value, deposition rates began to be measured above the detection limit. The four successful tests that measured deposition of MS2 reacting with free chlorine for 3 mg/L_0 × sec ranged from 0 Hz/hr to 7.45 Hz/hr with an average value of 3.93 Hz/hr and standard deviation of 3.22. The four successful tests that measured deposition of MS2 reacting with free chlorine for 8 mg/L_0 × sec ranged from 5.04 Hz/hr to 6.84 Hz/hr with an average value of 5.87 Hz/hr and standard deviation of 0.81. The seven successful tests at 14 mg/L_0 × sec ranged from 0 Hz/hr to 12.96 Hz/hr with an average value of 6.73 Hz/hr and

standard deviation of 4.62. Finally, the three successful tests at 20 mg/L_0 × sec ranged from 3.24 Hz/hr to 4.32 Hz/hr with an average value of 3.85 Hz/hr and standard deviation of 0.55. Figure 16 summarizes these results.

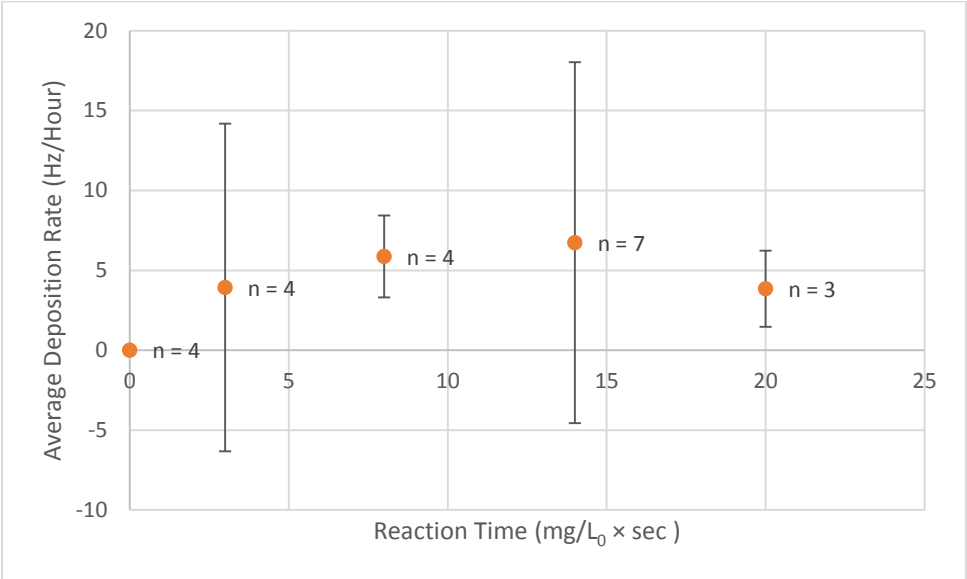

Figure 16: Plot comparing average MS2 deposition rates for different RT × $[FC]_0$ values. Error bars show 95% t-distribution based confidence interval.

Trends were difficult to decipher as the reaction time with free chlorine increased. There does not seem to be a monotonic relationship between reaction time and deposition rate. When comparing the data sets collected for the different contact times using the Student's t-test, a significant difference was found between deposition rates of MS2 reacting with free chlorine for 0 mg/L_0 × sec compared to 8, 14, and 20 mg/L_0 × sec. However, there was no calculated significant difference between deposition rates collected for RT × $[FC]_0$ values greater than 0 mg/L_0 × sec, with the exception of a calculated significant decrease in deposition rate from 8 to 20 mg/L_0 × sec. As shown in Table 8, most MS2 deposition rates with RT × $[FC]_0$ values greater

than 0 mg/L_0 × sec were significantly greater than 0 mg/L_0 × sec, with the exception of 3 mg/L_0 × sec.

RT × $[FC]^0$ (mg/L^0 × sec)	**0**	**3**	**8**	**14**	**20**
0		90.8%	99.9%	99.2%	99.3%
3	90.8%		68.1%	72.9%	3.6%
8	99.9%	68.1%		35.5%	98.9%
14	99.2%	72.9%	35.5%		84.7%
20	99.3%	3.6%	98.9%	84.7%	

Table 8: MS2 deposition rates after reacting with free chlorine for a specific RT × $[FC]_0$ value were compared with the Student's t-test (2-tails). *A 95.0% chance of a difference was assumed to be significant. Significant differences between deposition rates were highlighted in green. Insignificant differences were highlighted in red.*

The observation of no clear trend between the RT × $[FC]_0$ value and deposition hints at a complex relationship that most likely results from a series of reactions between free chlorine and the capsid structure that both increase and decrease forces of attraction between the MS2 particles and the silica surface. In general, a significant increase in deposition was observed when MS2 reacted with chlorine from an RT × $[FC]_0$ value of 0 mg/L_0 × sec to most values greater than 0 mg/L_0 × sec. There was no clear increase or decrease in deposition as the RT × $[FC]_0$ value continued to increase.

3.3.2 Deposition versus log_{10} Inactivation

Inactivation of MS2 was also recorded for each test and used as another criteria to analysis potential relationships and perhaps more accurately show how MS2 deposition is affected by reacting with free chlorine. The level of inactivation was not able to be measured for 7 of the 32 acceptable tests due to errors in executing the double layer plating method. Log_{10} inactivation levels from 0 to 11 were measured for the successful conducted tests. MS2 experiencing log_{10} inactivation levels increasing from 0 to 4 were assumed to have steadily accumulative structural damage to the virus structure. For any log_{10} inactivation reaching log_{10} 5 or higher, the MS2 virus was assumed to have experienced an equal amount of structural damage as observed by Wigginton et al., and these tests were consolidated into a single data set. Deposition was calculated and expressed as Hz/hr. Results were averaged for each log_{10} inactivation value and compared using the Student's t-test. Figure 17 below shows all of the collected data.

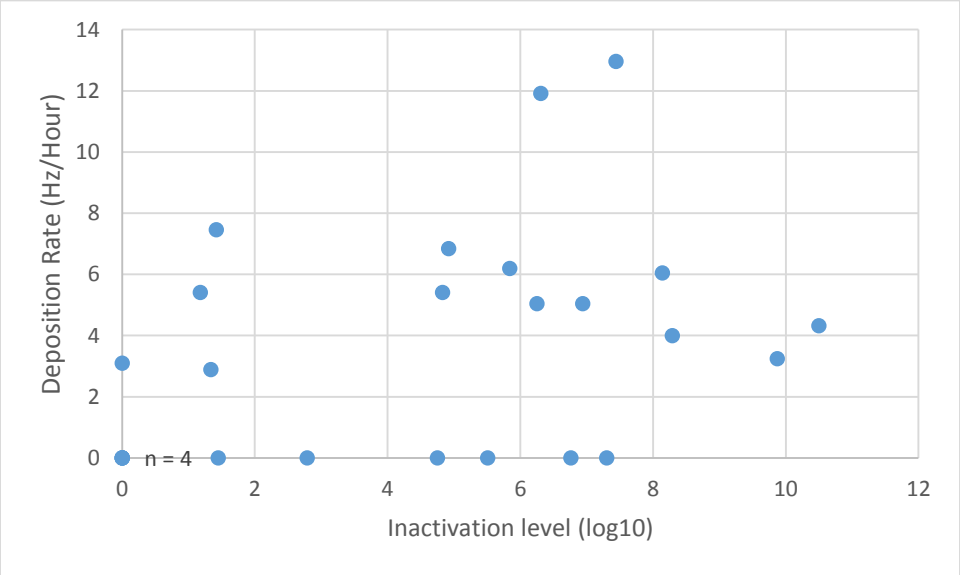

Figure 17: Plot comparing MS2 deposition rates for different log_{10} inactivation.

The four successful tests that measured MS2 deposition rates for test solutions experiencing 0 $\log_{10}$ inactivation all measured no deposition similar to what was observed for MS2 test solutions that did not react with chlorine. The four successful tests that measured MS2 deposition rates for test solutions experiencing 1 $\log_{10}$ inactivation had deposition rates ranging from 0 Hz/hr to 7.45 Hz/hr, with an averaged 3.39 Hz/hr, standard deviation of 3.22. The fifteen successful tests that measured MS2 deposition rates for test solutions experiencing 5 $\log_{10}$ inactivation or greater had deposition rates ranging from 0 Hz/hr to 12.96, with an averaged 4.73 Hz/hr, standard deviation of 3.97. Figure 18 summarizes these results.

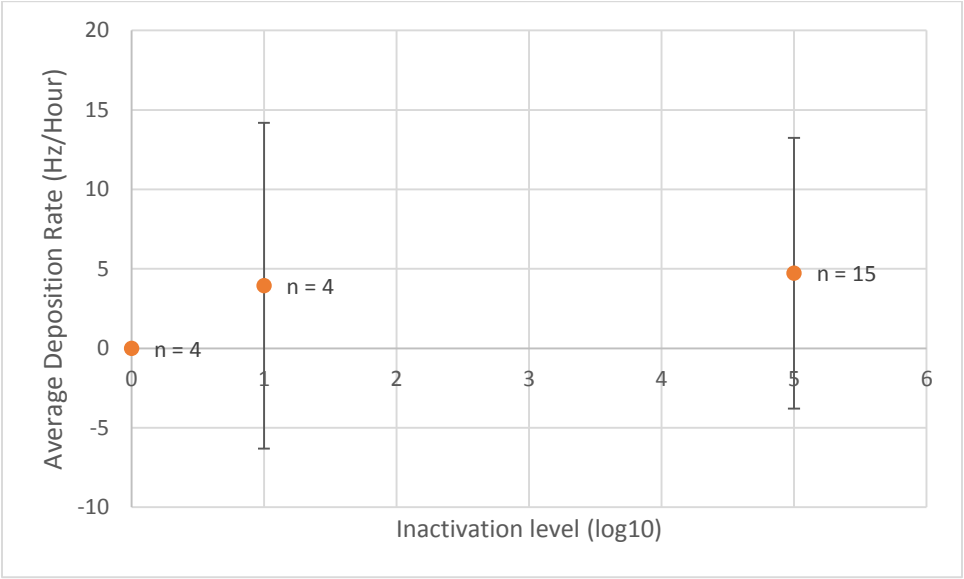

Figure 18: Plot comparing average MS2 deposition rates for different $\log_{10}$ inactivation. *Error bars show 95% t-distribution based confidence interval.*

Trends were again difficult to observe as the effect of $\log_{10}$ inactivation increased. However, this maybe have been due to the lack of data covering the range of inactivation between 2 and 4 $\log_{10}$. Comparing the data sets collected in Table 9 for the different $\log_{10}$ inactivation levels using the Student's t-test, only the deposition rate of MS2 test solutions

experiencing 5 $\log_{10}$ inactivation and greater was significant greater than the deposition rate of MS2 test solutions experiencing 0 $\log_{10}$ of inactivation. No significant difference was calculated between MS2 test solutions experiencing 0 $\log_{10}$ inactivation and 1 $\log_{10}$ inactivation, as well as between 1 $\log_{10}$ inactivation and 5 $\log_{10}$ inactivation. This again suggests that the relationship between MS2 deposition behavior and how much it has been oxidized by free chlorine is complex, most likely because of the complicated series of reactions with free chlorine and the various parts of the MS2 capsid structure. In general, an increase in deposition was observed after the MS2 test solution reacted with free chlorine at any level of exposure, but no trend was decipherable with further structural damage and inactivation.

Log_{10} Inactivation	**0**	**1**	**≥5**
0		90.8%	100%
1	90.8%		31.0%
≥5	100%	31.0%	

Table 9: MS2 deposition rates after experiences different $\log_{10}$ inactivation levles once reacting with free were compared with the Student's t-test (2-tails). *A 95.0% chance of a difference was assumed to be significant. Significant differences between deposition rates were highlighted in green. Insignificant differences were highlighted in red.*

3.3.3 Discussion of Results

Overall, a net increase in MS2 deposition rates was observed after reacting with free chlorine. However, there was no identifiable direct trend relationship as the extent of the reaction increased. This could potentially be explained by the reaction between the free chlorine and MS2 virus ceasing once the chlorine demand is met or the initial concentration of free chlorine is exhausted. However, this does not seem likely because the $\log_{10}$ inactivation of the test solution

continued to increase as the product value between initial concentration and contact time increased. A more likely cause is the complex set of molecular reactions previously studied between free chlorine and the various exposed capsid protein amino acids.

Electrostatic forces would not be expected to affect the deposition behavior in this situation because oxidation does not change the net charge of the amino acid structures, and electrostatic forces are most likely negated by the high ionic strength of the buffers solution. The net increase in deposition is likely caused by cross-linking and fragmentation. Cross-linking leads to aggregation and the creation of larger particles. Larger particles would have greater density, causing them to settle and possibly increase deposition onto the sensor surface. Fragmentation, though most likely inactivating the virus, would create smaller particles, potentially creating greater surface area and points of interaction with the sensor surface. The widespread oxidation of the protein backbone can lead to cross-linking and unfolding/fragmentation. The oxidation of tyrosine also leads to cross-linkages. In addition, an increase in the particle's hydrophobicity caused by the oxidation of methionine, cysteine (according to Vogt et al.), and tyrosine would also promote aggregation, and thus increased deposition.

Observing no identifiable direct trend relationship between the extent of the reaction and MS2 deposition hints that some molecular reactions may be interfering with increased deposition. Reactions causing the virus particle to become more hydrophilic would create a greater concentration of water molecules around the particle, preventing interaction with other surfaces and impede deposition. As explained before, the oxidation of the alpha and N-terminal amino groups on either end of the polypeptide chain creates polar aldehyde functional groups, thus making the virus particle more hydrophilic. The oxidation of lysine also leads to more

hydrophilic products. However, because of the net increase in the rate of MS2 deposition, it seems that these reactions with the alpha and N-terminal amino groups and lysine do not influence the deposition behavior of MS2 as much as the oxidation of methionine, cysteine, and tyrosine and the extensive oxidation of the protein backbone.

Chapter 4: Conclusions

This study aimed to better understand how oxidative stress from both natural and unnatural sources affects the transport behavior of viruses through groundwater and sand filtration processes. The study involved using MS2 bacteriophage as a surrogate virus, free chlorine supplied as sodium hypochlorite to provide the oxidative stress, and a silica coated sensor to mimic a soil surface. Deposition data was collected on a QCM-D to provide advanced precision.

Measurable MS2 deposition on the QCM-D was optimized by improving the purity of the MS2 stock compared to similar studies. Test solutions spiked with an MS2 stock that was purified with the FPLC process seemed to have much less deposition compared to test solutions with the same concentration of MS2 but spiked with a stock not purified with the FPLC process. These observation suggest that strong consideration over purification methodology should be taken when measuring MS2 deposition on a QCM-D. Because of its high sensitivity, background substances must be removed to ensure accurate data.

This study also attempted to characterize the effect of free chlorine oxidation on MS2 deposition behavior. A net increase in MS2 deposition rates was observed after reacting with free chlorine. As the reaction increased in magnitude, there was no identifiable direct correlation with deposition rate as measured deposition seemed to fluctuation between 0 and 10 Hz/hr. This behavior was explained to potentially be caused by the complex set of reactions between the free

chlorine and the various amino acid structures located on the exterior of the virus capsid protein. Although we only studied chlorine, it suggests that oxidation changes behavior. Based on these observations, it is expected that virus contaminated water exposed to free chlorine would contain less viruses after flowing through the subsurface or through a sand filter compared to contaminated water not exposed to free chlorine. Exposure to free chlorine promotes deposition, allowing subsurface soil particles and sand filters to remove more virus particles. This would produce groundwater and sand filter filtrate of a higher purity.

This study proved to be challenging in several aspects. Using the QCM-D to analyze the deposition kinetics of microorganisms is a very meticulous and lengthy process. Extensive cleaning of all the components is critical to comprehensible measurements. Impurities in the chamber or tubes can affect data collection and make it difficult to establish a baseline. All components of the QCM-D, including the sensors, deteriorate and lose their integrity overtime. It is often difficult to differentiate between deposition and interference as the frequency noise increases with every use of a sensor. The amorphous nature of microorganisms compared to inorganic particles also contributes to the inconsistency within the data, which is further magnified by the advanced sensitivity of the QCM-D. All of these factors made it difficult to consistently conduct acceptable tests.

There are several means to progress further in studying the influence of oxidative stress on viral deposition. More tests can be conducted to verify how the presence of impurities in virus stocks jeopardize the soundness of measured deposition, further validating the importance of extensive purification processes such as FPLC. It would also be useful to conduct a comparative study using an experimental technique other than QCM-D, such as sand columns, to further verify the observations in this study. Finally, even though bacteriophage MS2 is a widely used

surrogate virus, it does have several very unique characteristics such as its strong negative electrostatic charge, its hydrophobic exterior, and the hydrophilic polypeptide loops that protrude from the capsid structure. In general, MS2 adsorption to soil is low compared to most other viruses (Jin, Yates, Thompson, & Jury, 1997), so the validity of MS2 as a surrogate virus can be questioned. A supplemental study analyzing the effect of free chlorine oxidation on a different virus would greatly assist in developing a comprehensive understanding. Similarly, conducting similar studies using other types of oxidants such as ultra violet light, singlet oxygen, and ozone would be useful.

Bibliography

American Public Health Association, American Water Works Association, Water Environment Federation. (2005). *Standard Methods for the Examination of Water & Wastewater* (21 ed.). Washington, D.C.

Amino Acids. (2013, March 31). Retrieved from Biochematics: https://biochemanics.wordpress.com/2013/03/31/amino-acids/

Bacteriophage MS2 (MS2). (2015). Retrieved from Virus Particle Explorer (VIPERdb): http://viperdb.scripps.edu/index.php

Balke, K.-D., & Zhu, Y. (2008, March). Natural water purification and water management by artificial groundwater recharge. *Journal of Zhejiang University-SCIENCE B, 9*(3), 221–226. Retrieved from http://www.ncbi.nlm.nih.gov/pmc/articles/PMC2266879/

Berger, P., & Zoller , U. (1994). *Ground Water Contamination and Control.* New York: Marcel Dekker.

Berlett, B., & Stadtman, E. (1997, August 15). Protein oxidation in aging, disease, and oxidative stress. *The Journal of Biological Chemistry, 272*(33), 20313-20316. Retrieved from http://www.ncbi.nlm.nih.gov/pubmed/9252331

Biolin Scientific. (2012, August 1-2). QCM-D Basic Training Course. Linthicum Heights, Maryland, USA.

Biolin Scientific. (2014). *Q-Sense*. Retrieved from Biolin Scientific: http://www.biolinscientific.com/q-sense/

Böhlke, J.-K. (2002, February). Groundwater recharge and agricultural contamination. *Hydrogeology Journal, 10*(1), 153-179. Retrieved from http://link.springer.com.proxy-um.researchport.umd.edu/article/10.1007/s10040-001-0183-3

Brewer, S., Glomm, W., Johnson, M., Knag, M., & Franzen, S. (2001, May 29). Probing BSA Binding to Citrate-Coated Gold Nanoparticles. *Journal of Membrane Science, 194*, 69-79.

Brinton, C., Gemski, P., & Carnahan, J. (1964, September). A NEW TYPE OF BACTERIAL PILUS GENETICALLY CONTROLLED BY THE FERTILITY FACTOR OF E. COLI K 12 AND ITS ROLE IN CHROMOSOME TRANSFER. *Proceedings of the National Academy of Sciences of the United States of America, 52*, 776-796. Retrieved from http://www.ncbi.nlm.nih.gov/pubmed/14212557

Centers for Disease Control and Prevention. (2009, December 29). *Guideline for Disinfection and Sterilization in Healthcare Facilities*. Retrieved from Centers for Disease Control and Prevention: http://www.cdc.gov/hicpac/Disinfection_Sterilization/6_0disinfection.html

Centers for Disease Control and Prevention. (2010, May 7). *Healthy Swimming/Recreational Water: Chlorine Disinfection Timetable: Timetable for killing common illness-causing germs*. Retrieved from Centers for Disease Control and Prevention Web site: http://www.cdc.gov/healthywater/swimming/pools/chlorine-disinfection-timetable.html

Centers for Disease Control and Prevention. (2013, November 19). *Hepatitis A Information for the Public: Hepatitis A FAQs for the Public*. Retrieved from Centers for Disease Control and Prevention Web site: http://www.cdc.gov/hepatitis/A/aFAQ.htm

Chao, C., Ma, Y., & Stadtman, E. (1997, April 1). Modification of protein surface hydrophobicity and methionine oxidation by oxidative systems. *Proceedings of the National Academy of Sciences, 94*(7), 2969–2974. Retrieved from http://www.pnas.org/content/94/7/2969.short

Cliver, D. O., & Moe, C. L. (2004). *Waterborne Zoonoses.* London, UK: World Health Organization.

Dawson, D., Paish, A., Staffell, L., Seymour, I., & Appleton, H. (2005, Januaray). Survival of viruses on fresh produce, using MS2 as a surrogate for norovirus. *Journal of Applied Microbiology, 98*(1), 203-209. Retrieved from http://www.ncbi.nlm.nih.gov/pubmed/15610433

Debbink, K., Lindesmith, L. C., Donaldson, E. F., & Baric, R. S. (2012, October 18). Norovirus Immunity and the Great Escape. *PLOS Pathogens, 8*(10). Retrieved from http://www.ncbi.nlm.nih.gov/pmc/articles/PMC3475665/

Donahue, R., Miller, R., & Shi, J. (1977). *Soils: an introduction to soils and plant growth.* Prentice-Hall.

Dubinina, E. E., Gavrovskaya, S. V., Kuzmich, E. V., Leonova, N. V., Morozova, M. G., Kovrugina, S. V., & Smirnova, T. A. (2002, March). Oxidative Modification of Proteins: Oxidation of Tryptophan and Production of Dityrosine in Purified Proteins Using Fenton's System. *Biochemistry, 67*(3), 343-350. Retrieved from http://link.springer.com/article/10.1023/A:1014840617890

Farkas, K., Varsani, A., & Pang, L. (2014, October 24). Adsorption of Rotavirus, MS2 Bacteriophage and Surface-Modified Silica Nanoparticles to Hydrophobic Matter. *Food and Environment Virology*, Epub ahead of print.

Fetter, C. (1999). *Contaminant Hydrogeology.* Prentice Hall.

Fu, S. (2000, March 30). Reactions of Hypochlorous Acid with Tyrosine and Peptidyl-tyrosyl Residues Give Dichlorinated and Aldehydic Products in Addition to 3-Chlorotyrosine. *Journal of Biological Chemistry, 275*(15), 10851-10858. Retrieved from http://www.jbc.org/cgi/doi/10.1074/jbc.275.15.10851

Golmohammadi, R., Valegård, K., Fridborg, K., & Liljas, L. (1993, December 5). The refined structure of bacteriophage MS2 at 2.8 A resolution. *Journal of Molecular Biology, 234*(3), 620-639. Retrieved from http://www.ncbi.nlm.nih.gov/pubmed/8254664?dopt=Abstract

Hawkins, C. L., & Davies, M. J. (2005, September 21). Inactivation of Protease Inhibitors and Lysozyme by Hypochlorous Acid: Role of Side-Chain Oxidation and Protein Unfolding in Loss of Biological Function. *Chemical Research in Toxicology, 18*(10), 1600-1610. Retrieved from http://pubs.acs.org/doi/abs/10.1021/tx050207b

Hawkins, C., & Davies, M. (1998a). Reaction of HOCl with amino acids and peptides: EPR evidence for rapid rearrangement and fragmentation reactions of nitrogen-centred radicals. *Journal of the Chemical Society*, 1937-1946. Retrieved from http://pubs.rsc.org/en/content/articlehtml/1998/p2/a802949k

Hawkins, C., & Davies, M. (1998b). Hypochlorite-induced damage to proteins: formation of nitrogen-centred radicals from lysine residues and their role in protein fragmentation. *Biochemical Journal, 332*, 617–625. Retrieved from http://www.biochemj.org/bj/332/bj3320617.htm

Hoff, J. C. (1986). *Inactivation of microbial agents by chemical disinfectants.* Cincinnati, OH: Environmental Protection Agency. Retrieved from http://www.who.int/water_sanitation_health/dwq/en/watreatpath.pdf

Jakob, U., Muse, W., Eser, M., & Bardwell, J. (1999, February 5). Chaperone activity with a redox switch. *Cell, 96*(3), 341-352. Retrieved from http://www.sciencedirect.com/science/article/pii/S0092867400805474

Jin, Y., Yates, M. V., Thompson, S. S., & Jury, W. A. (1997). Sorption of Viruses during Flow through Saturated Sand Columns. *Environmental Science and Technology, 31*(2), 548–555. Retrieved from http://pubs.acs.org/doi/abs/10.1021/es9604323

Laskowski, J., & Kitchener, J. (1969, April). The hydrophilic—hydrophobic transition on silica. *Journal of Colloid and Interface Science, 29*(4), 670–679. Retrieved from http://www.sciencedirect.com.proxy-um.researchport.umd.edu/science/article/pii/0021979769902197

Loveland, J., Ryan, J., Amy, G., & Harvey, R. (1996, February 20). The reversibility of virus attachment to mineral surfaces. *Colloids and Surfaces A: Physicochemical and Engineering Aspects, 107*(20), 205–221. Retrieved from http://www.sciencedirect.com/science/article/pii/0927775795033734

Loveland, J., Ryan, J., GL, A., & RW, H. (1996, February 20). The reversibility of virus attachment to mineral surfaces. *Colloids and Surfaces A: Physicochemical and Engineering Aspects, 107*, 205–221. Retrieved from http://www.sciencedirect.com/science/article/pii/0927775795033734

Mattle, M. J., Crouzy, B., Brennecke, M., Wigginton, K. R., Perona, P., & Kohn, T. (2011, August 5). Impact of Virus Aggregation on Inactivation by Peracetic Acid and Implications for Other Disinfectants. *Environmental Science and Technology, 45*(18), 7710–7717. Retrieved from http://pubs.acs.org/doi/abs/10.1021/es201633s

McGraw-Hill Education. (n.d.). *Chapter 27: Amino Acids, Peptides and Proteins*. Retrieved from McGraw-Hill Higher Education: http://www.mhhe.com/physsci/chemistry/carey5e/Ch27/ch27-1-4-2.html

Michen , B., & Graule , T. (2010, August). Isoelectric points of viruses. *Journal of Applied Microbiology, 109*(2), 388-397. Retrieved from http://www.ncbi.nlm.nih.gov/pubmed/20102425

Narang, H., & Codd, A. (1981, May). Frequency of preclumped virus in routine fecal specimens from patients with acute nonbacterial gastroenteritis. *Journal of Clinical Microbiology, 13*(5), 982-988. Retrieved from http://www.ncbi.nlm.nih.gov/pmc/articles/PMC273927/

Ogata, N. (2007, April 24). Denaturation of Protein by Chlorine Dioxide: Oxidative Modification of Tryptophan and Tyrosine Residues. *Biochemistry, 46*(16), 4898-4911. Retrieved from http://pubs.acs.org/doi/abs/10.1021/bi061827u

Ophardt, C. E. (2003a). *Characteristics and Properties of Amino Acids*. (Elmhurst College) Retrieved from Virtual Chembook: http://www.elmhurst.edu/~chm/vchembook/561aminostructure.html

Ophardt, C. E. (2003b). *Polarity of Organic Compounds*. (Elmhurst Collage) Retrieved from Virtual Chembook: http://www.elmhurst.edu/~chm/vchembook/213organicfcgp.html

Pattison, D. I., Hawkins, C. L., & Davies, M. J. (2007, August 3). Hypochlorous Acid-Mediated Protein Oxidation: How Important Are Chloramine Transfer Reactions and Protein Tertiary Structure? *Biochemistry, 46*(34), 9853–9864. Retrieved from http://pubs.acs.org/doi/abs/10.1021/bi7008294

Pattison, D. I., & Davies, M. J. (2001, October). Absolute Rate Constants for the Reaction of. *Chemical Research in Toxicology, 14*(10), 1453-1464. Retrieved from http://www.ncbi.nlm.nih.gov/pubmed/11599938

Pecson, B. M., Martin, L. V., & Kohn, T. (2009, September). Quantitative PCR for Determining the Infectivity of Bacteriophage MS2 upon Inactivation by Heat, UV-B Radiation, and Singlet Oxygen: Advantages and Limitations of an Enzymatic Treatment To Reduce False-Positive Results. *Applied and Environmental Microbiology, 75*(17), 5544–5554. Retrieved from http://www.ncbi.nlm.nih.gov/pubmed/19592538

Penrod, S., Olson, T., & Grant, S. (1996, November 13). Deposition kinetics of two viruses in packed beds of quartz granular media. *Langmuir, 12*(23), 5576–5587. Retrieved from http://pubs.acs.org/doi/abs/10.1021/la950884d

Proteins. (2007-2015). Retrieved from Peptide Guide: http://www.peptideguide.com/proteins.html

Rechendorff, K., Hovgaard, M., Foss, M., Zhdanov, V., & Besenbacher, F. (2006, November 2). Enhancement of Protein Adsorption Induced by Surface Roughness. *Langmuir, 22*, 10885-10888.

Russel, W., Saville, D., & Schowalter , W. (1992). *Colloidal dispersions.* Cambridge University Press.

Shields , P. A., & Farrah, S. R. (2002, August). Characterization of Virus Adsorption by Using DEAE-Sepharose and Octyl-Sepharose. *Applied and Environmental Microbiology, 68*(8), 3965-3968. Retrieved from http://aem.asm.org/content/68/8/3965.short

Stadtman, E. (1992, August 28). Protein oxidation and aging. *Science, 257*(5074), 1220-1224. Retrieved from http://www.sciencemag.org/content/257/5074/1220.short

Standard Methods for the Examination of Water and Wastewater, 14th Ed. (1975). In *Method 409F, "DPD Colorimetric Method"* (p. 332).

Steinmann, J. (2004, April). Surrogate viruses for testing virucidal efficacy of chemical disinfectants. *Journal of Hospital Infection, 56*(2), 49–54. Retrieved from http://www.sciencedirect.com/science/article/pii/S0195670103005188

Tate, J., Burton , A., Boschi-Pinto, C., Steele , A., Duque , J., Parashar , U., & WHO-coordinated Global Rotavirus Surveillance Net. (2012, February). 2008 estimate of worldwide rotavirus-associated mortality in children younger than 5 years before the introduction of universal rotavirus vaccination programmes: a systematic review and meta-analysis. *The Lancet Infectious Diseases, 12*(2), 136-141. Retrieved from http://www.ncbi.nlm.nih.gov/pubmed/22030330

The UniProt Consortium. (2015). UniProt: a hub for protein information. Retrieved from http://www.uniprot.org/

Tong, M., Shen, Y., Yang, H., & Kim, H. (2012, April 1). Deposition kinetics of MS2 bacteriophages on clay mineral surfaces. *Colloids and Surfaces B: Biointerfaces, 92*, 340–347. Retrieved from http://linkinghub.elsevier.com/retrieve/pii/S0927776511007569

US Environmental Protection Agency. (1975). Standard Methods for the Examination of Water and Wastewater. *Method 409F, "DPD Colorimetric Method", 14*, 332.

Valegård, K., Liljas, L., Fridborg, K., & Unge, T. (1990, May 3). The three-dimensional structure of the bacterial virus MS2. *Nature, 345*(6270), 36-41. Retrieved from http://www.ncbi.nlm.nih.gov/pubmed/2330049

Vogt, W. (1995, January). Oxidation of methionyl residues in proteins: Tools, targets, and reversal. *Free Radical Biology and Medicine, 18*(1), 93–105. Retrieved from http://www.sciencedirect.com/science/article/pii/089158499400158G

Voorthuizen, E., Ashbolt, N., & Schäfer, A. (2001, November 30). Role of hydrophobic and electrostatic interactions for initial enteric virus retention by MF membranes. *Journal of Membrane Science, 194*(1), 69–79. Retrieved from http://www.sciencedirect.com/science/article/pii/S0376738801005221

Vörös, J. (2004, July). The Density and Refractive Index of Adsorbing Protein Layers. *Biophysical Journal, 87*(1), 553-561. Retrieved from http://www.ncbi.nlm.nih.gov/pmc/articles/PMC1304376/

Walse, S. S., Plewa, M. J., & Mitch, W. A. (2009, September 15). Exploring Amino Acid Side Chain Decomposition Using Enzymatic Digestion and HPLC-MS: Combined Lysine Transformations in Chlorinated Waters. *Analytical Chemistry, 81*(18), 7650-7659. Retrieved from http://www.ncbi.nlm.nih.gov/pubmed/19691274

Wigginton, K. R., & Kohn, T. (2012, February). Virus disinfection mechanisms: the role of virus composition, structure, and function. *Virus entry/Environmental virology, 2*(1), 84–89. Retrieved from http://www.sciencedirect.com.proxy-um.researchport.umd.edu/science/article/pii/S1879625711001684

Wigginton, K. R., Pecson, B. M., Sigstam, T., Bosshard, F. B., & Kohn, T. (2012, October 26). Virus Inactivation Mechanisms: Impact of Disinfectants on Virus Function and Structural Integrity. *Environmental Science & Technology, 46*(21), 12069–12078. Retrieved from http://pubs.acs.org/doi/abs/10.1021/es3029473

Winter, T., Harvey, J., Franke, O., & Alley, W. (2013). *Ground Water And Surface Water A Single Resource.* U.S. Geological Survey , U.S. Department of the Interior. Retrieved from http://pubs.usgs.gov/circ/circ1139/

World Health Organization. (2014, October). *Media Center: Poliomyelitis*. Retrieved from World Health Organization Web site: http://www.who.int/mediacentre/factsheets/fs114/en/

Yuan, B., Pham, M., & Nguyen, T. H. (2008, October 15). Deposition Kinetics of Bacteriophage MS2 on a Silica Surface Coated with Natural Organic Matter in a Radial Stagnation Point Flow Cell.

Environmental Science & Technology, 42(20), 7628-7633. Retrieved from http://pubs.acs.org/doi/abs/10.1021/es801003s

Zhang, C., & Vetelino, J. (2003, June). Chemical sensors based on electrically sensitive quartz resonators. *Sensors and Actuators B: Chemical, 91*(1-3), 320–325. Retrieved from http://www.sciencedirect.com.proxy-um.researchport.umd.edu/science/article/pii/S0925400503000947